Bachelor thesis

Steady-state Analytical Investigation of a Passive Closed Loop Cooling Cycle for the Emergency Drain Tank of a Molten Salt Reactor

by

F. Roos

Delft University of Technology

15 December 2022

Thesis committee:	prof. dr. ir. J. L. Kloosterman,	TU Delft, supervisor
	dr. ir. D. Lathouwers	TU Delft, co-supervisor

TU Delft

Abstract

The emergency drain tank (EDT) is safety feature for the molten salt reactor (MSR). If the fuel-salt overheats, or in the event of a power breakdown, a freeze-plug melts and the fuel-salt enters the emergency drain tank. The fuel-salt releases decay-heat and should be cooled towards the operating temperature (725 °C). The cooling process should prevent the fuel-salt from boiling (1755 °C), and prevent the hastelloy-N casing of the EDT from melting ($1250-1350$ °C). In the proposed cooling cycle heat is generated in the EDT and drained in a heat-exchanger. First a visual model for the closed loop is constructed. Secondly the model is defined mathematically by making use of a buoyancy - friction relation, a thermodynamic balance and the closed loop constraints. Lastly a `scipy.optimize.fsolve` based algorithm is used to solve for the coolant mass-flow rate and the EDT in-/outlet temperature. Desirable solutions are a high mass-flow rate and low in-/outlet temperatures. Solutions are calculated as function of the spatial loop parameters: the chimney height, the horizontal loop length and the heat-exchanger length. And the thermodynamic parameters: the heat transfer coefficient and the external temperature of the heat-exchanger. The process is repeated for different coolants: Propyleneglycol with a mass-flow rate of 40 kg/s and temperatures close to 4.0×10^2 K, water with a mass-flow rate of 31 kg/s and temperatures close to 4.0×10^2K, carbon dioxide with a mass-flow rate of 2.3 kg/s and temperatures close to 5.0×10^2K and 1.0×10^3K, and air with a low mass-flow rate of 1.4 kg/s and in-/outlet temperatures 3.5×10^2K and 1.3×10^2K respectively. The parameters that influence the solutions the most are the heat transfer coefficient and the heat-exchanger length

Contents

Nomenclature

α	thermal diffusivity ($m^2\ s^{-1}$)
$\mathfrak{h}$	specific enthalpy ($J\ kg^{-1}\ kg^{-1}$)
$\mathfrak{Q}$	internal heat production (J)
μ	dynamic viscosity ($kg^2\ m^{-4}\ s^{-1}$)
ν	kinematic viscosity ($J\ kg^{-1} s$)
ρ	density (kg/m^3)
τ	pressure ($kg\ m^{-1}\ s^{-2}$)
A	cross sectional area (m^2)
c_p	specific heat capacity ($J\ kg^{-1}\ K^{-1}$)
D_h	hydraulic diameter (m)
f	Darcy friction factor (-)
g	gravitational constant (m/s^2)
h	heat transfer coefficient ($W\ m^{-2}\ K^{-1}$)
k	thermal conductivity ($W\ m^{-1}\ K^{-1}$)
L_c	characteristic length (m)
m	mass-flow rate (kg/s)
p	pressure (kg m-1s-2)
P_w	wet perimeter (m)
Q	heat transfer rate (W)
q''	heat flux (J/m^2)
T	temperature (K)
t	time (s)
u	specific internal energy ($J\ kg^{-1}$)
v	velocity (m/s)

List of Figures

List of Tables

1

Introduction

1.1. Previous work

Molten salts reactors (MSRs) make use of a liquid salt in which fission, fertile and fissile material is dissolved. The molten salt acts as fuel and as coolant within the nuclear reactor. Within the MSR the fuel salt flows through the reactor after which it is transferred to the primary heat-exchanger where the heat is transferred to a secondary molten salt coolant. The cooled fuel-salt enters the reactor again and the process repeats itself, as shown in figure 1.1. Within the reactor graphite control rods act as moderator which slow down high velocity neutrons in order to increase the likely hood of fission [1]. Other types of MSRs are also studied. The molten salt fast reactor (MSFR) for instance, does not make use of a solid moderator [2]. The different types of MSRs do however all need an adequate safety system that cools and/or stores the fuel-salt if the fuel-salt overheats and/or the nuclear power plant loses power for some reason. One of the safety features in the MSR design is the freeze-plug and corresponding emergency drain tanks (EDTs).

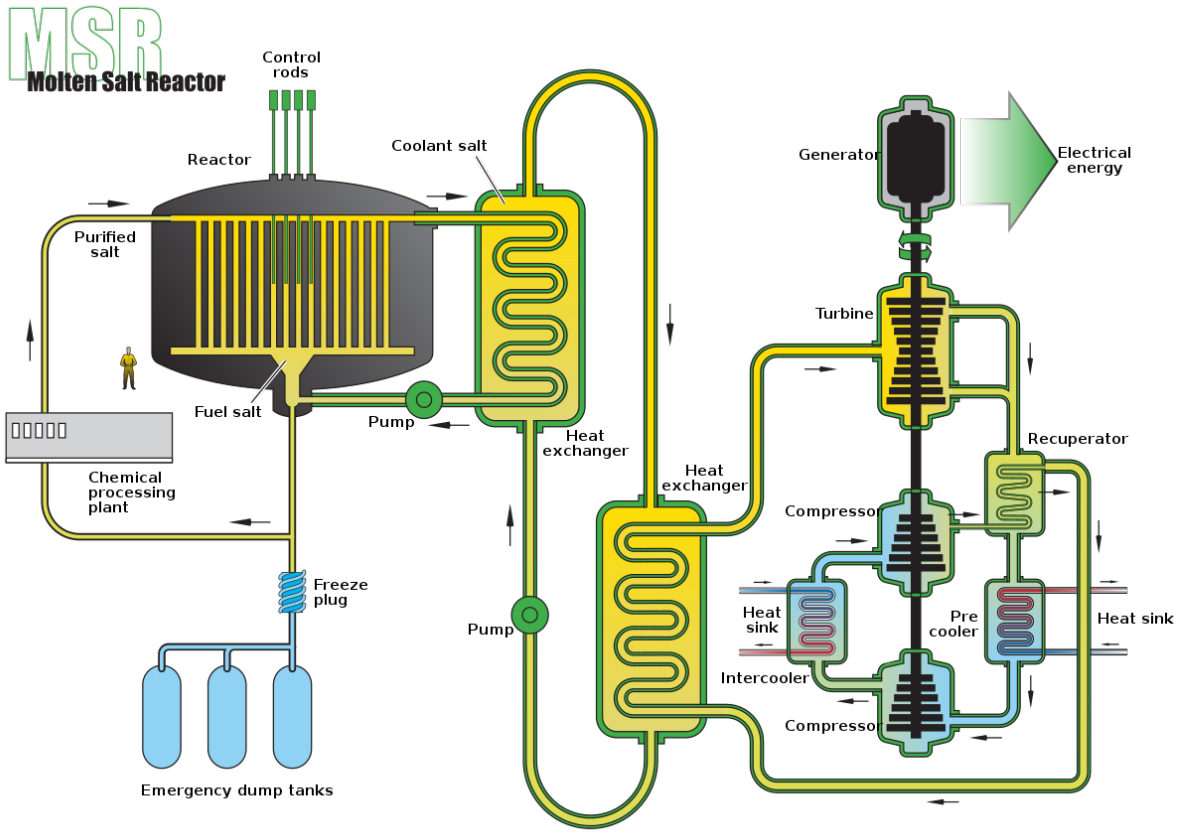

Figure 1.1: Molten salt reactor with fuel/coolant salt loop, freeze-plug and emergency dump/drain tanks [1].

Within the design of the MSR the EDT system is an important safety feature. When the fuel-salt overheats within the reactor it should be drained towards the EDT, and cooled. Both the drainage and cooling system should work passively, meaning that no external interference is needed to drain the fuel salt. Between the reactor and EDT, which structure is shown in figure 1.2a, a so called freeze-plug is

located which melts when the reactor overheats, or when the system that cools the freeze-plug fails. Because of the fact that the EDT is located below the reactor the fuel-salt will than drain towards the EDT due to gravity, and therefore passively. For the EDT a hexagon shaped drain tank has been suggested [3][4]. The EDT consists of a number of smaller hexagons unit cells, a single unit cell is illustrated in figure 1.2b. The unit-cell consists of an outer fuel-salt layer, a metal casing, an inert-salt layer, another metal casing and a coolant in the center.

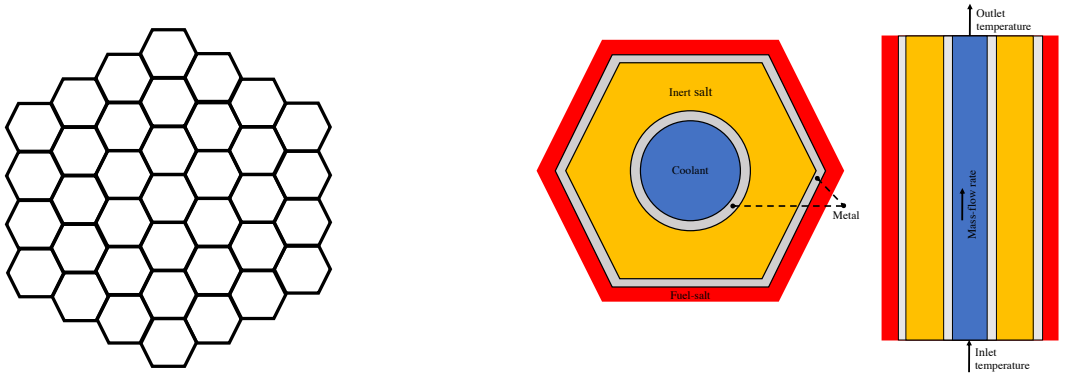

(a) Structure of hexagonal EDT, top view.

(b) Structure of EDT unit cell, top view.

Figure 1.2: Structures of EDT and unit cell, top view.

When the fuel-salt enters the EDT it generates a fraction of the nominal-power $Q_{\text{tot.}}$ in the form of decay-heat. Because of the decay-heat, the fuel-salt will keep heating up if there is no adequate cooling mechanism. The goal of the EDT, on a short time scale, is to keep the fuel-salt below its boiling point, which is around $1755°\text{C}$. When hastelloy-N the limiting factor becomes the melting point of the nickel based alloy, which is in the $1250-1350°\text{C}$ range [5]. To make sure that the fuel-salt does not boil and the hastelloy-N does not melt, the fuel-salt should be cooled fast enough to prevent this critical rise in temperature. But, cooling the fuel-salt too fast will produce an isolating layer of frozen fuel-salt at the outer-border of the outer metal-shell. On a longer time-scale the fuel-salt should be cooled towards a safe operating temperature so it can again be reused in the reactor. The MSFR reactor proposed in the SAMOFAR project operates at a temperature of $725°\text{C}$.

Within the EDT the amount of decay-heat produced by the fuel-salt will decrease as a function of time and is defined as: $Q_{\text{th.}}(t) = \chi(t)Q_{\text{tot.}}$, where $\chi(t)$ is defined as the decay-heat fraction. The decay-heat fraction is an empirically[1] determined relation that is shown in figure 1.3. The decay-heat fraction will vary over time from: $\chi(t = 1\text{s}) \approx 6.2\%$, to $\chi(t = 10 \text{ days}) \approx 0.3\%$. The decay-heat will be most intense during the first 0.1 days (2.4 hours). Within this time span of 2.4 hours the decay-heat will decrease, from its initial 6.2%, to approximately 1%. An adequate cooling system should be able to process the peak capacity during the first hours, and ensure appropriate cooling on the longer time scale in the order of: 10 days.

[1]The decay-heat fraction $\chi(t)$ is not strictly empirical, the relation can be determined mathematically by taking the sum of the individual exponential decay terms of the fission products.

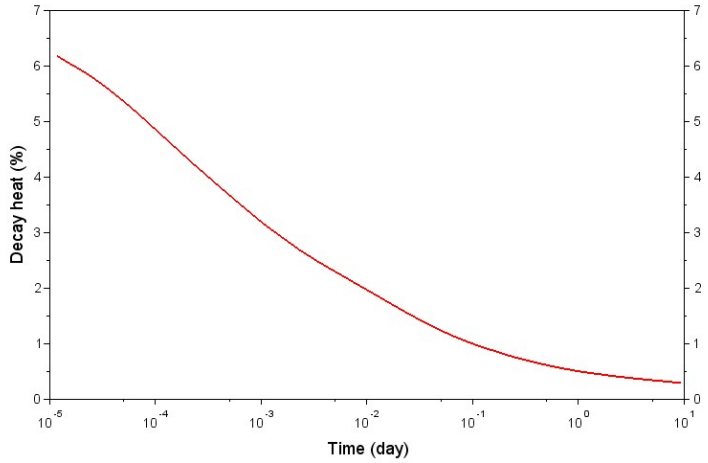

Figure 1.3: Decay-heat fraction as function of time [4].

Within previous work by C.Péniguel [6] a system was suggested, with the geometry described in figure 1.2, where the coolant of choice was air; the metal was chosen to be hastelloy-N. Within the air cooled system, the inlet temperature of the air would be 20°C, the velocity of the flowing air would be 1 m/s. The system was modeled as a function of time using different heat transfer coefficients. Complications would arise when the heat transfer coefficients were chosen similar to that of an air circuit, the temperature of the different materials: fuel-salt, inert-salt and hastelloy-N would keep on increasing.

1.2. Current project

The suggested unit-cell geometry has been used as a starting point for further modelling. To study the behaviour of different coolants, a closed loop cooling cycle has been chosen with a number of parameters and in steady-state. The loop will transport the coolant from the EDT towards a heat-exchanger, in which it is cooled. Using this closed loop model, an analytical model is used to describe the flow of the coolant and its temperature profile within the loop. The analytical model is used to construct an algorithm which calculates the mass-flow rate and the inlet temperature of the coolant. The solutions for the mass-flow rate and the inlet temperature are fixed by the conditions caused by the loop model and are used for further evaluations.

The inlet temperature can be used to describe the outlet temperature, which is the temperature of the coolant that exits the EDT. To study the effect of using different parameters within the loop model, the input values of these parameters are altered one by one. The parameters that are studied are the heat transfer coefficient, the length and the external temperature of the heat-changer. Furthermore, the horizontal length of the closed loop will be studied. Chaining the coolant also gives different values for the mass-flow rate and the outlet temperature, this effect is studied as well. The effect of the parameters and different coolants will be displayed and discussed.

To understand the analytical relations that are constructed using the loop model, the physical theory

behind these relations is given in chapter two. Within this chapter the physical concepts for a flowing fluid will be treated, as well as the relations considering the temperature profile. Furthermore, the main type of heat transport will be discussed. The physical relations will be put to use in chapter three. Using a closed loop model, and the relations found in the previous chapter, specific physical solutions for the system will be determined. The physical solutions will be used to construct an algorithmic model that ensures solutions for the values of the mass-flow rate and the inlet/outlet temperature. with respect to the EDT. Chapter four, results, is dedicated to the solutions of the algorithm when different parameter values and coolant types are chosen. The results are discussed in chapter five, after which the study is concluded and recommendations are given in the sixth and final chapter.

2

Theoretical background

2.1. Governing equations concerning the flow

Using the Navier Stokes equations for the conservation of mass and momentum a flow can be described. The equations are evaluated for a system which is in steady-state and by making use of a number of simplifications. The results are further evaluated using the Boussinesq approximation, and a closed loop condition. These steps lead to a workable formula which can be used for analytical purposes. The used symbols are explained in the Nomenclature.

2.1.1. Navier-Stokes equations for the conservation of mass and momentum

A flowing fluid can be represented using the Navier Stokes[1]. The continuity equation represents the conservation of mass and is formulated as the expression shown in equation 2.1:

$$\frac{\partial \rho}{\partial t} + \frac{1}{A}\vec{\nabla} \cdot \vec{m} = 0. \tag{2.1}$$

The conservation of momentum can be represented by equation 2.2:

$$\frac{1}{A}\frac{\partial}{\partial t}(\vec{m}) + \frac{1}{\rho A^2}\vec{\nabla} \cdot (\rho \vec{m}\vec{m}) = -\nabla p + \vec{\nabla} \cdot \vec{\tau} + \rho \vec{g}. \tag{2.2}$$

Within a one-dimensional system that faces in the z-direction, the density ρ and the fluid velocity $\vec{v}$ are cross-sectional averages [7]. The direction of $\vec{v}$ will face entirely in the z-direction, and can therefore be expressed as v_z. Using this information, equation 2.1 can be expressed without the nabla operator $\vec{\nabla}$ and becomes:

$$\frac{\partial \rho}{\partial t} + \frac{1}{A}\frac{\partial \dot{m}_z}{\partial z} = 0, \tag{2.3}$$

which, in steady-state, becomes:

$$\frac{1}{A}\frac{\partial \dot{m}_z}{\partial z} = 0, \tag{2.4}$$

and therefore:

$$\frac{\partial \dot{m}_z}{\partial z} = 0. \tag{2.5}$$

When a closed loop is considered, the z-direction can be replaced by a loop parameter s which faces in the direction of the loop. Because of the fact that equation 2.5 is no longer a vector function, the equation can be rewritten in terms of the loop parameter by replacing z by s. This results in the following equation:

$$\frac{\partial \dot{m}_s}{\partial s} = 0. \tag{2.6}$$

The same holds for the conservation of momentum described in equation 2.2, this equation can be rewritten as:

$$\frac{1}{A}\frac{\partial \dot{m}_z}{\partial t} + \frac{1}{\rho A^2}\frac{\partial \dot{m}_z^2}{\partial z} = -\frac{\partial p}{\partial z} - \rho \tilde{g} - \frac{1}{A}\oint_{P_w} \tau \, dP_w. \tag{2.7}$$

[1] The Navier Stokes equation for the conservation of energy is discussed in section 2.2 equations. The entire derivation is provided using the steps described in [7], which is a more detailed and complete derivation.

The first three terms in equation 2.7 are rewritten in a scalar differential form. Furthermore, it is assumed that the only friction is caused by the walls in contact with the fluid. The friction term τ can therefore be rewritten as a loop integral with respect to the walls. The friction term will evaluate to:

$$\oint_{P_w} \tau \, dP_w = f \frac{\dot{m}_z^2}{2 D_h A \rho}. \tag{2.8}$$

Using this relation equation 2.7 will become:

$$\frac{1}{A}\frac{\partial \dot{m}_z}{\partial t} + \frac{1}{\rho A^2}\frac{\partial \dot{m}_z^2}{\partial z} = -\frac{\partial p}{\partial z} - \rho \tilde{g} - f \frac{\dot{m}_z^2}{2 D_h A^2 \rho}, \tag{2.9}$$

which in steady-state becomes:

$$\frac{1}{\rho A^2}\frac{\partial \dot{m}_z^2}{\partial z} = -\frac{\partial p}{\partial z} - \rho \tilde{g} - f \frac{\dot{m}_z^2}{2 D_h A^2 \rho}. \tag{2.10}$$

Equation 2.10 can be written in terms of s using the same considerations that led to equation 2.6. This results in the following equation:

$$\frac{1}{\rho A^2}\frac{\partial \dot{m}_s^2}{\partial s} = -\frac{\partial p}{\partial s} - \rho \tilde{g} - f \frac{\dot{m}_s^2}{2 D_h A^2 \rho}. \tag{2.11}$$

2.1.2. The Boussinesq approximation

Within a system where mass, momentum and energy are conserved, which is derived in section 2.1.1, and temperature differences occur as function of the position; the Boussinesq approximation [8] can be used to simplify, in this case, equation 2.10. The approximation states that variation in fluid properties, except for the fluid density ρ, can be ignored. Furthermore, it is stated that the only non-constant density terms are those which are multiplied by the gravitational constant operator $\tilde{g}$. The constant density terms will be expressed as a reference density ρ_0, the non-constant density terms will become:

$$\rho = \rho_0 \big[1 - \beta\big(T(s) - T_0\big)\big]. \tag{2.12}$$

Evaluating equation 2.10 using the approximation described in equation 2.12 results in:

$$\frac{1}{\rho A^2}\frac{\partial \dot{m}_s^2}{\partial s} = -\frac{\partial p}{\partial s} - \rho_0 \big[1 - \beta\big(T(s) - T_0\big)\big]\tilde{g} - f \frac{\dot{m}_s^2}{2 D_h A^2 \rho_0}, \tag{2.13}$$

using equation 2.5 the left-hand side of equation 2.13 will evaluate to zero[2] and become:

$$-\frac{\partial p}{\partial s} - \rho_0 \big[1 - \beta\big(T(s) - T_0\big)\big]\tilde{g} = f \frac{\dot{m}_s^2}{2 D_h A^2 \rho_0}. \tag{2.14}$$

A further simplification can be made when a closed loop system is considered in the x and z-direction. To fit both directions, which are assumed to be independent and to never change at the same time (the fluid will always flow in the x or the z-direction, not in a combination of both directions), both directions are fitted into the loop parameter s. Using this parameter, the gravitational constant operator $\tilde{g}$ can be written as a scalar for all the four possible directions of the mass-flow rate $\dot{m}$:

[2] When the derivative of p is zero, the derivative of p^2 will also be zero using the chain/product-rule [9].

Table 2.1: Orientation of gravitational constant as function of mass-flow rate rate direction.

Mass-flow rate direction	Value of $\tilde{g}$
$+\hat{z}$	$+g$
$-\hat{z}$	$-g$
$+\hat{x}$	0
$-\hat{x}$	0

The terms given in table 2.1 can be fitted into one expression where $\tilde{g}$ is replaced by the dot product: $g(\hat{z}\cdot\hat{s})$. Using the loop-parameter s, and its consequences, equation 2.14 can be rewritten as:

$$\frac{\partial p}{\partial s}+\rho_0\big[1-\beta\big(T(s)-T_0\big)\big]g(\hat{z}\cdot\hat{s})=-f\frac{\dot{m}_s^2}{2D_hA^2\rho_0} \tag{2.15}$$

When s forms a closed loop, and equation 2.15 is integrated with respect to s, the equation will evaluate to:

$$\oint_s\frac{\partial p}{\partial s}ds+\oint_s\rho_0\big[1-\beta\big(T(s)-T_0\big)\big]g(\hat{z}\cdot\hat{s})ds=\oint_s-f\frac{\dot{m}_s^2}{2D_hA^2\rho_0}ds, \tag{2.16}$$

the pressure-term: $\oint_s\frac{\partial p}{\partial s}ds$ will evaluate to zero [10] and equation 2.16 will become:

$$\oint_s\rho_0\big[1-\beta\big(T(s)-T_0\big)\big]g(\hat{z}\cdot\hat{s})ds=\oint_s-f\frac{\dot{m}_s^2}{2D_hA^2\rho_0}ds. \tag{2.17}$$

2.2. Governing equations concerning the thermodynamics

The Navier stokes equation for the conservation of energy is evaluated for a system in steady-state. By making use of several simplifications the equation can be written as a compact formula which can be used for analytical purposes. Further on, convective heat transport will be discussed. Convective heat transport forms the main type of heat transport when fluids are considered. The used symbols are explained in the Nomenclature.

2.2.1. Navier Stokes equation for energy conservation

The Navier Stokes[3] equation for the conservation of energy [7] is described by:

$$\frac{\partial}{\partial t}(\rho u)+\vec{\nabla}\cdot\rho u\vec{v}=-\vec{\nabla}\cdot\vec{q}''+\dot{\Omega}-\vec{\nabla}\cdot p\vec{v}+\vec{\nabla}\cdot(\vec{\tau}\cdot\vec{v})+\vec{v}\cdot\rho\vec{g}. \tag{2.18}$$

This equation is reduced into one dimension. When there is no internal heat generation and friction is negligible, the following relation remains:

$$A\frac{\partial\rho u}{\partial t}+\frac{\partial A\rho v_x\left(u+\frac{p}{\rho}\right)}{\partial x}=q'. \tag{2.19}$$

Using the fact that the part within the brackets can be rewritten as the specific enthalpy $\mathfrak{h}$, the following one dimensional equation remains:

$$A\frac{\partial\rho\mathfrak{h}}{\partial t}+\frac{\dot{m}\mathfrak{h}}{\partial x}=q'+A\frac{\partial p}{\partial t}, \tag{2.20}$$

[3]The entire derivation is provided using the steps described in [7], which is a more detailed and complete derivation.

which in steady-state becomes:

$$\frac{d(\dot{m}\mathfrak{h})}{dx} = q'. \tag{2.21}$$

The specific enthalpy can be rewritten as function [11] of the specific heat capacity and the temperature: $d\mathfrak{h} = c_\mathrm{p} dT$. Using this expression for the specific enthalpy, and a simplification that states that the mass-flow $\dot{m}$ will not depend on the position x, the following equation remains:

$$\dot{m}\frac{d\left(c_\mathrm{p} T\right)}{dx} = q'. \tag{2.22}$$

The specific heat capacity will be a function of T (and therefore a function of the loop parameter s), by replacing the specific heat capacity term by an average specific heat capacity: $\langle c_\mathrm{p} \rangle$ the term can be taken out of the differential. Furthermore, equation 2.22 can be written in terms of s using the same considerations that led to equation 2.6, and 2.11. This results in the following equation:

$$\dot{m}\langle c_\mathrm{p} \rangle \frac{dT}{ds} = q'. \tag{2.23}$$

2.2.2. Convective heat transport

Within the field of thermodynamics, Newton's law of cooling states that a temperature difference ΔT ensures a heat transfer rate Q between two, or more, bodies which are in contact. The direction of the heat transfer rate faces from a hot object towards a colder object. Furthermore, the heat transfer rate is directly proportional to the temperature difference and scaled by the average heat transfer coefficient $\langle h \rangle$ and the area of the body A. This results in the relation presented in equation 2.24:

$$Q = \langle h \rangle A \Delta T(t). \tag{2.24}$$

The relation shown in equation 2.24 applies only for convective heat transport, and therefore for flowing fluids [12]. Convective heat transport can be split into free convection and forced convection, a combination of both is also possible. Forced convection is considered to be non passive, an external source forces a fluid to move along an object. Free, or natural, convection is considered to be a passive process where density, pressure and temperature differences induce buoyancy effects which makes a fluid flow naturally [13]. Within the field of convective heat transport the average Nusselt number $\langle Nu \rangle$ can be introduced, which can be expressed as a function [14] of the heat transfer coefficient h:

$$\langle Nu \rangle = \frac{1}{L_c}\int_0^{L_c} \frac{h_x dx L_c}{k} = \frac{\langle h \rangle L_c}{k}, \tag{2.25}$$

where L_c and k are defined as the characteristic length and thermal conductivity respectively. The characteristic length L_c for a fluid that flows through a pipe will be the diameter of the pipe D. Therefore equation 2.25 can be written as:

$$\langle Nu \rangle = \frac{\langle h \rangle D}{k}, \tag{2.26}$$

for a fluid that flows through a pipe. Equation 2.26 can be rewritten to the form:

$$\langle h \rangle = \frac{\langle Nu \rangle k}{D}. \tag{2.27}$$

The Nusselt number can be rewritten as a function of a set dimensionless numbers through empirical relations, depending on the considered geometry. For free convective heat transport the average Nusselt number will typically be a function of the Rayleigh Ra, and the Prandtl Pr number: $f(Ra, Pr)$. If the dominant type of heat transfer is considered to be forced convection, the average Nusselt number can be rewritten as a function of at least the Reynolds Re and the Prandtl Pr number: $f(Re, Pr)$. Both functions depend on the considered system, and are found through experimental studies. The Prandtl number can be described as:

$$Pr = \frac{c_\mathrm{p}\mu}{k}, \tag{2.28}$$

the Reynolds number as:

$$Re = \frac{\rho v L_c}{\mu}, \tag{2.29}$$

and the Rayleigh number can be described as:

$$Ra = \frac{g\beta c_\mathrm{p}}{\nu\alpha}\Delta T L_c^3. \tag{2.30}$$

3

Model description

3.1. Visual model representation

The model can be divided into three sub-models. First a visual model is constructed using a EDT unit-cell as starting point. Around this unit-cell a loop will be constructed and visualised. The visualisation is used to define variables, parameters and constants within the model. The visual model will form a basis for the mathematical evaluation of the model. The mathematical expressions will be used in an algorithm which calculates the variables presented within the visual model.

3.1.1. The emergency drain tank

The emergency drain tank consists of a number of hexagonal unit-cells. The total volume of fuel-salt that enters the EDT is $V_{\text{tot.}}$. The total fission power of this fuel-salt is $Q_{\text{tot.}}$. The total amount of decay-heat is: $Q_{\text{th.}}$, which is a fraction of $Q_{\text{tot.}}$ and defined as: $Q_{\text{th.}} = Q_{\text{tot.}}\chi(t)$. When a single hexagonal unit-cell is considered, the amount of heat produced per unit length can be calculated using equation 3.1:

$$q'_{\text{th.}} = Q'''_{\text{th.}} A_{\text{fuel-salt}} = \frac{Q_{\text{th.}}}{V_{\text{tot.}}} A_{\text{fuel-salt}} = \chi(t) \frac{Q_{\text{tot.}}}{V_{\text{tot.}}} A_{\text{fuel-salt}}. \tag{3.1}$$

Using the geometry and dimensions shown in figure 3.1, equation 3.1 can be written as:

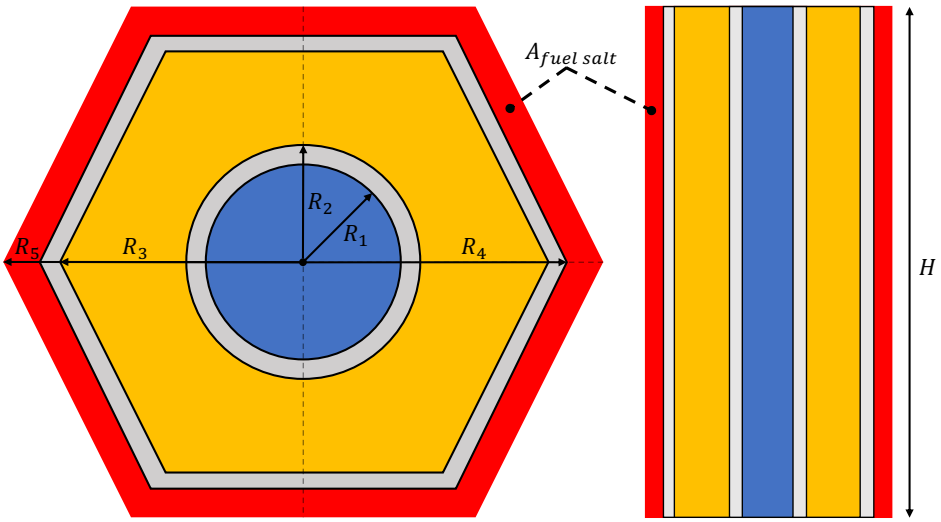

Figure 3.1: The EDT unit cell, with a horizontal cross section top view (left) and a vertical cross section side view (right). Including dimensions.

where the $A_{\text{fuel-salt}}$ term can be expressed using the two outer radii of the hexagon [15]:

$$q'_{\text{th.}} = \chi(t) \frac{Q_{\text{tot.}}}{V_{\text{tot.}}} \left(R_5^2 - R_4^2\right) \frac{3\sqrt{3}}{2}. \tag{3.2}$$

Equation 3.2 is the work formula used to calculate the amount of heat produced per unit length, per unit-cell. The exact values of H, R_1, R_4, R_5, $V_{\text{tot.}}$ and $Q_{\text{tot.}}$ are given in Appendix C.

3.1.2. The closed loop cooling cycle

To cool the fuel-salt layer of a unit-cell, presented in figure 3.1, a closed loop model is used. The coolant flows through a closed loop with mass-flow rate $\dot{m}_s$. The coolant will heat up in the EDT and cooled down in the heat-exchanger. This model is illustrated in figure 3.2:

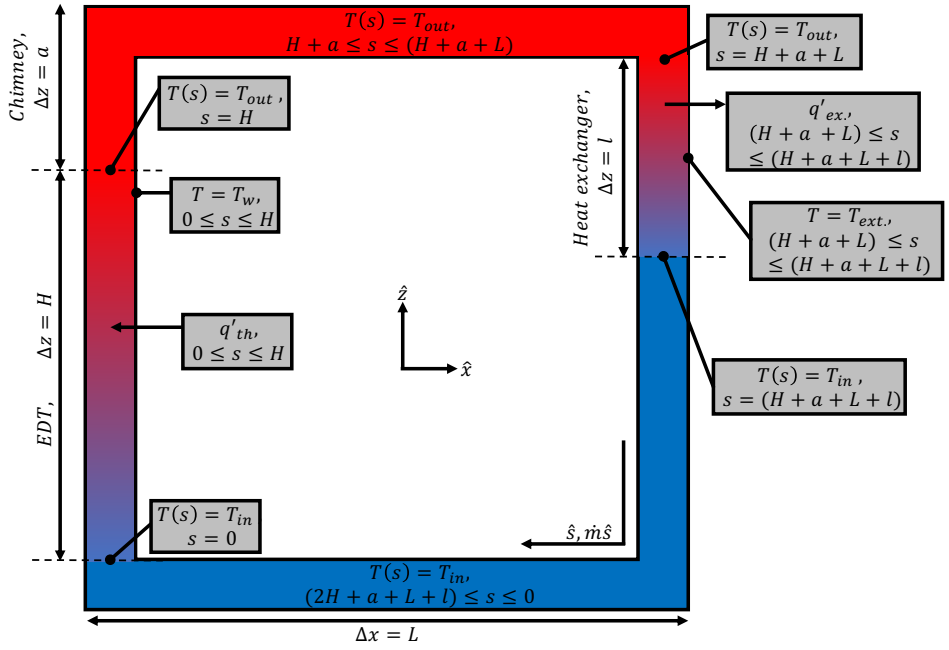

Figure 3.2: Closed loop model including EDT unit cell and heat exchanger.

Within the closed loop, s stands for the loop parameter which faces parallel to the mass-flow rate $\dot{m}_s$. The loop parameter and mass-flow rate always face in a direction parallel to the direction of the loop in a clockwise way. The height of the unit-cell H, shown in figure 3.1 (right), is considered to be a constant within the model. The amount of heat per unit length that enters the loop through the EDT is $q'_{\text{th.}}$, which is defined and bound by the decay-heat fraction presented in figure 1.3. The other part which adds height to the loop is the chimney length a, which is chosen to be a parameter within the model. The horizontal length of the model is a parameter called L. The length of the heat-exchanger l, is also a parameter and is chosen so that $0 < l \leq (H + a)$ is true. The amount of heat per unit length that exits the loop through the heat-exchanger is $q'_{\text{ex.}}$, this is a function of the external temperature $T_{\text{ext.}}$ and the heat transfer coefficient h of the heat-exchanger which are both considered to be parameters. The pipe diameter D is considered to be a constant, and the same, within the entire loop. The coolant temperature at $s = 0$ is a variable called T_{in}, the temperature will rise as function of T_{in} and $q'_{\text{th.}}$ within the EDT towards T_{out} and remain constant from $s = H$ to $s = H + a + L$, where it will enter the heat-exchanger. Within the heat-exchanger the coolant should be cooled to T_{in} again to form a closed loop.

3.2. Analytical model

The visual model is used, in combination with the thermodynamic and flow equations, to construct a mathematical model. The mathematical model can be divided into a first part where the temperature as function of the loop parameter s can be evaluated. And a second part where the buoyancy - friction relation, presented in section 2.1.2, can be evaluated using the analytic results of the thermodynamic relation. The analytical model will form a basis for the algorithmic model which is used for further calculations.

3.2.1. Thermodynamic relation

The system is considered to be in steady-state. Temperature differences will therefore only depend on the position s within the loop and are a function of the heat production term $q'_{\text{th.}}$, and extraction term $q'_{\text{ex.}}$. Therefore the following equation remains to be solved:

$$\dot{m}_s \langle c_\text{p} \rangle \frac{dT}{ds} = q'_{\text{th.}} + q'_{\text{ex.}}, \tag{3.3}$$

In order to solve equation 3.3 analytically, $q'_{\text{th.}}$ is chosen to be independent of s and uniformly distributed over the EDT unit cell height H. Furthermore, the heat-exchanger term $q'_{\text{ex.}}$ can be written as a function of the heat-transfer coefficient h and a temperature difference ΔT using Newton's law of cooling. Equation 3.3 can therefore be rewritten as:

$$\dot{m}_s \langle c_\text{p} \rangle \frac{dT}{ds} = q'_{\text{th.}} + hD\Delta T, \tag{3.4}$$

which, when using $T_{\text{ext.}}$, becomes:

$$\dot{m}_s \langle c_\text{p} \rangle \frac{dT}{ds} = q'_{\text{th.}} + hD\big[T(s) - T_{\text{ext.}}\big]. \tag{3.5}$$

Because of the fact that both parts of equation 3.5 are independent[1] the solution of equation 3.5 becomes a combination the differential equations which are to be solved. The first part evaluates to:

$$T(s) = \frac{q'_{\text{th.}}}{\dot{m}_s \langle c_\text{p} \rangle} s + T_{\text{in}}, \tag{3.6}$$

which is the solution for: $s \in \big[0, H\big]$. Equation 3.6 can be used to express T_{out} in terms of T_{in}. The outlet temperature will be equation 3.6 evaluated for $s = H$. The second solution therefore becomes:

$$T_{\text{out}} = \frac{q'_{\text{th.}}}{\dot{m}_s \langle c_\text{p} \rangle} H + T_{\text{in}}, \tag{3.7}$$

which is the solution for: $s \in \big[H, H + a + L\big]$. The third solution:

$$T(s) = T_{\text{ext.}} + \Big(T_{\text{out}} - T_{\text{ext.}}\Big) \exp\Big[\frac{hD}{\dot{m}_s \langle c_\text{p} \rangle}(H + a + L)\Big] \exp\Big[\frac{-hD}{\dot{m}_s \langle c_\text{p} \rangle} s\Big] \tag{3.8}$$

$$= T_{\text{ext.}} + \Big(\frac{q'_{\text{th.}}}{\dot{m}_s \langle c_\text{p} \rangle} H + T_{\text{in}} - T_{\text{ext.}}\Big) \exp\Big[\frac{hD}{\dot{m}_s \langle c_\text{p} \rangle}(H + a + L)\Big] \exp\Big[\frac{-hD}{\dot{m}_s \langle c_\text{p} \rangle} s\Big], \tag{3.9}$$

[1] The two heat-exchanging parts can be solved independently because they act on different parts of the loop. Because the system is a closed loop they do however provide each other with boundary conditions.

which is the solution for for: $s \in [H+a+L, H+a+L+l]$. And the fourth solution:

$$T(s) = T_{\text{in}}, \tag{3.10}$$

which is the solution for: $s \in [H+a+L+l, 2(H+a+L)]$. Because of the fact that a closed loop in steady-state is considered further conditions must be obeyed. The inlet-temperature T_{in} at position $s=0$ should, after passing through the EDT and the heat-exchanger, again be equal to T_{in} at position $s=2(H+a+L)$. This means that the absolute value of the temperature difference over the EDT: $|\Delta T_{\text{EDT}}|$ should equal the absolute temperature difference over the heat-exchanger: $|\Delta T_{\text{ex.}}|$. Which results in the following relation for the temperature differences:

$$|\Delta T_{\text{EDT}}| = |\Delta T_{\text{ex.}}| = \frac{q'_{\text{th.}}}{\dot{m}_s \langle c_{\text{p}} \rangle} H = (T_{\text{in}} - T_{\text{ext.}}) + \frac{q'_{\text{th.}}}{\dot{m}_s \langle c_{\text{p}} \rangle} H - \left(\frac{q'_{\text{th.}}}{\dot{m}_s \langle c_{\text{p}} \rangle} H + T_{\text{in}} - T_{\text{ext.}} \right) \exp\left[\frac{-hD}{\dot{m}_s \langle c_{\text{p}} \rangle} l \right], \tag{3.11}$$

which can be further simplified to:

$$(T_{\text{in}} - T_{\text{ext.}}) - \left(\frac{q'_{\text{th.}}}{\dot{m}_s \langle c_{\text{p}} \rangle} H + T_{\text{in}} - T_{\text{ext.}} \right) \exp\left[\frac{-hD}{\dot{m}_s \langle c_{\text{p}} \rangle} l \right] = 0. \tag{3.12}$$

3.2.2. Buoyancy - Friction relation

Using the Buoyancy - Friction relation presented in equation 2.17, the temperature relations found in equations 3.6 - 3.10 and the dimensions presented in figure 3.2, a second relation can be derived:

$$\oint_s -f \frac{\dot{m}_s^2}{2 D_h A \rho_0} ds = -f \frac{\dot{m}_s^2}{2 D_h A \rho_0} \int_0^{2(H+a+L)} ds = -f \frac{\dot{m}_s^2}{D_h A \rho_0} (H+a+L). \tag{3.13}$$

The left-hand side of equation 2.17 will evaluate [2] to:

$$\begin{aligned} \oint_s \rho_0 \left[1 - \beta\left(T(s) - T_0\right)\right] g(\hat{z} \cdot \hat{s}) ds = H \left[1 - \beta \left(0.5 \frac{q'_{\text{th.}}}{\dot{m}_s \langle c_{\text{p}} \rangle} H + (T_{\text{in}} - T_0) \right) \right] + a \left[1 - \beta \left(\frac{q'_{\text{th.}}}{\dot{m}_s \langle c_{\text{p}} \rangle} H + (T_{\text{in}} - T_0) \right) \right] - \\ l \left[1 - \beta (T_{\text{ext.}} - T_0) \right] + \beta \left(\frac{q'_{\text{th.}}}{\dot{m}_s \langle c_{\text{p}} \rangle} + (T_{\text{in}} - T_{\text{ext.}}) \right) \left(1 - \exp\left[\frac{-hD}{\dot{m}_s \langle c_{\text{p}} \rangle} l \right] \right) \frac{\dot{m}_s \langle c_{\text{p}} \rangle}{hD} + \\ \left[1 - \beta (T_{\text{in}} - T_0) \right] (l - H - a) \end{aligned} \tag{3.14}$$

When equations 3.13 and 3.14 are combined, and the hydraulic diameter D_h is chosen to be the pipe diameter D (which is assumed to be the same within the entire loop presented in figure 3.2 and defined as $D = 2R_1$), the following relation remains:

$$\begin{aligned} -f \frac{\dot{m}_s^2}{D A \rho_0} (H+a+L) = H \left[1 - \beta \left(0.5 \frac{q'_{\text{th.}}}{\dot{m}_s \langle c_{\text{p}} \rangle} H + (T_{\text{in}} - T_0) \right) \right] + a \left[1 - \beta \left(\frac{q'_{\text{th.}}}{\dot{m}_s \langle c_{\text{p}} \rangle} H + (T_{\text{in}} - T_0) \right) \right] - \\ l \left[1 - \beta (T_{\text{ext.}} - T_0) \right] + \beta \left(\frac{q'_{\text{th.}}}{\dot{m}_s \langle c_{\text{p}} \rangle} + (T_{\text{in}} - T_{\text{ext.}}) \right) \left(1 - \exp\left[\frac{-hD}{\dot{m}_s \langle c_{\text{p}} \rangle} l \right] \right) \frac{\dot{m}_s \langle c_{\text{p}} \rangle}{hD} + \\ \left[1 - \beta (T_{\text{in}} - T_0) \right] (l - H - a) \end{aligned} \tag{3.15}$$

The expression that is used to calculate the Darcy friction factor is: $f = 0.0056 + 0.5 Re^{-0.32}$ which is an empirical relation for turbulent pipe flows [16].

[2] The complete derivation of equation 3.14 is given in appendix A.

3.3. Algorithmic model and data generation

To solve equations 3.12 and A.8, an algorithm in `Python` is used. The strategy is to determine the roots of system of equations formed by equations 3.12 and A.8 using a `SciPy` [17] root solving module in `Python`. The following two dimensional functions are therefore introduced:

$$f(\dot{m}_s, T_{\text{in}}) = (T_{\text{in}} - T_{\text{ext.}}) - \Big(\frac{q'_{\text{th.}}}{\dot{m}_s\langle c_{\text{p}}\rangle} H + T_{\text{in}} - T_{\text{ext.}}\Big) \exp\Big[\frac{-hD}{\dot{m}_s\langle c_{\text{p}}\rangle} l\Big], \tag{3.16}$$

and

$$\begin{aligned} g(\dot{m}_s, T_{\text{in}}) = f\frac{\dot{m}_s^2}{DA\rho_0}(H + a + L) + H\Big[1 - \beta\Big(0.5\frac{q'_{\text{th.}}}{\dot{m}_s\langle c_{\text{p}}\rangle} H + (T_{\text{in}} - T_0)\Big)\Big] + \\ a\Big[1 - \beta\Big(\frac{q'_{\text{th.}}}{\dot{m}_s\langle c_{\text{p}}\rangle} H + (T_{\text{in}} - T_0)\Big)\Big] - l\big[1 - \beta(T_{\text{ext.}} - T_0)\big] + \\ \beta\Big(\frac{q'_{\text{th.}}}{\dot{m}_s\langle c_{\text{p}}\rangle} + (T_{\text{in}} - T_{\text{ext.}})\Big)\Big(1 - \exp\Big[\frac{-hD}{\dot{m}_s\langle c_{\text{p}}\rangle} l\Big]\Big)\frac{\dot{m}_s\langle c_{\text{p}}\rangle}{hD} + \\ \big[1 - \beta(T_{\text{in}} - T_0)\big](l - H - a) \end{aligned} \tag{3.17}$$

The two functions f and g are presented to the `scipy.optimize.fsolve` module in a vector of the form: $[f, g]$. Within the functions the variables $\dot{m}_s$ and T_{in} are vectorized to the form: $[\dot{m}_s, T_{\text{in}}]$, which will be named the standard-form. Furthermore, an initial-guess for both variables has to be presented to the algorithm, schematically displayed in figure 3.3, in standard-form: $[\dot{m}_{s_{\text{guess}}}, T_{\text{in}_{\text{guess}}}]$ in order for the algorithm to work. The `scipy.optimize.fsolve` has a broad range of parameters that can be used to gain more control over the process, the parameters that are used in the algorithm are: the tolerance (chosen at 1×10^{-11}), which ensures that the algorithm will terminate if the relative error between two consecutive is at most the chosen tolerance, and the factor (chosen at 0.1) which determines the initial step bound. The result will be a variable solution vector in standard-form: $[\dot{m}_{s_{sol}}, T_{\text{in}_{sol}}]$. The output solutions are an approximation so that $f(\dot{m}_{s_{sol}}, T_{\text{in}_{sol}}) \approx 0$ and $g(\dot{m}_{s_{sol}}, T_{\text{in}_{sol}}) \approx 0$ (in the order of 10^{-6}, which is a is a realistic and small error in the proposed algorithm). The solutions $[\dot{m}_{s_{sol}}, T_{\text{in}_{sol}}]$ are checked for validity by filling them back into the functions f and g, these outputs should be approximately zero. If the system of equations has multiple roots, the solution output will be the solution which is closed to the initial guess $[\dot{m}_{s_{\text{guess}}}, T_{\text{in}_{\text{guess}}}]$. The algorithm that is used by the `scipy.optimize.fsolve` module, is a modification of the Powell hybrid method called the `MINPACK subroutine HYBRJ` [18]. This is an irritative method which calculates and uses the Jacobian of the function to determine the roots of an arbitrary large system of equations. The `Python` code used to calculate the solutions $\dot{m}_s$ and T_{in} of functions f and g is presented in appendix B.

To generate data, the code is used to evaluate the effect of different coolants and parameters. The strategy is to chose a coolant and determine a set of reference solutions with a fixed set of parameters. After finding reference solutions the individual parameters are systematically altered in value. The values of interest will be the variable solution of $\dot{m}_s$ for different parameters and T_{out}, which is a function of the variable solution T_{in} as described in equation 3.7. Solutions that are desirable are those which

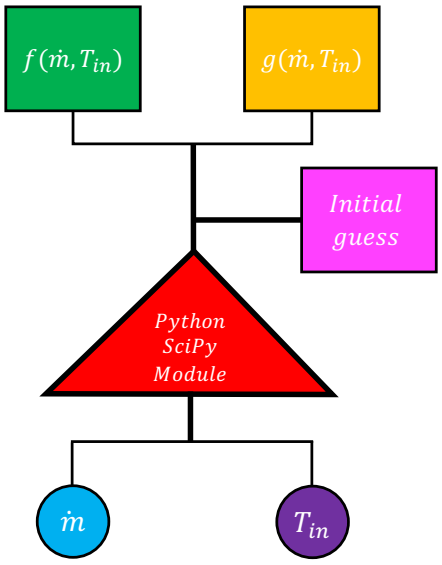

Figure 3.3: Visual representation of the algorithmic model.

ensure a high mass-flow rate $\dot{m}_s$, and a low inlet/outlet temperature T_{in} and T_{out} respectively. After altering the set of individual parameters, the effect of altering multiple parameters at the same time is studied. This process is repeated for a number of other coolants. Within the process of data generation, the decay-heat fraction $\chi(t)$ will be fixed at its peak value. When a coolant is considered, the degree of freedom is the choice of parameter values. The parameter values will be altered using an iterative process which ensures a set of solutions of functions f and g. These solutions can be represented as a function: $p(A)$ where the parameter that is altered is: A. Changing multiple parameters: A, B at the same time will result in a function: $p(A, B)$.

4

Results

4.1. Air cooled system

First a system using air as a coolant is studied. The physical properties of air are taken at the reference temperature $T_0 = 20°C$ (293 K), a pressure of 1 bar and with no moisturisation. This results in the following properties [19]:

Table 4.1: Physical constants air.

Constant	**Symbol**	**Unit**	
Reference temperature	T_0	K	293
Reference density	ρ_0	kg/m^3	1.2
Specific heat capacity	c_p	J/kgK	1.0×10^3
Thermal expansion coefficient	β	K^{-1}	3.4×10^{-3}
Dynamic viscosity	μ	Pas	1.8×10^{-5}

4.1.1. Reference solutions

To gain insight in the effect of different parameters, a reference solution is calculated for the maximum amount of decay-heat 6.2%, which is equivalent to: 0.19 GW. Within this reference solution the following parameter values are chosen:

Table 4.2: Reference parameters air.

Parameters	**Symbol**	**Unit**	
Horizontal length	L	m	3
Chimney length	a	m	17
Heat Exchanger length	l	m	20
Heat transfer coefficient	h	W/m^2K	30
External temperature	$T_{ext.}$	K	293

The heat transfer coefficient of 1.0×10^2 W/m^{2}K (which is a value higher than that of an air to air circuit proposed by C.Péniguel) is used to give generate solutions that are more realistic. Using a very low heat transfer coefficient makes the values of T_{in} and T_{out} rise towards infinity. For the reference solution the chimney length a is chosen to be 17m. The chimney height has been chosen to be a realistic value, choosing smaller values gives unrealistic solutions for T_{in} and T_{out}. Choosing bigger values leaves less space to compare the reference results to an upper limit for the chimney height, that has to be realistic as well. The external temperature $T_{\text{ext.}}$ is chosen to be at room temperature. The length of the heat-exchanger l is chosen to be the maximal length allowed when using $a = 17$. Lastly, the horizontal length L is chosen to be the same as the height of the EDT within the reference solution. These choices result in the following reference solutions:

Table 4.3: Reference solutions air.

Variable	**Symbol**	**Unit**	
Mass-flow rate	$\dot{m}$	kg/s	1.4
Inlet temperature	T_{in}	K	2.2×10^3
Outlet temperature	T_{out}	K	3.1×10^3

Using the reference parameters, the reference solutions as function of the decay-heat fraction $\chi(t)$ can be determined, these are the following:

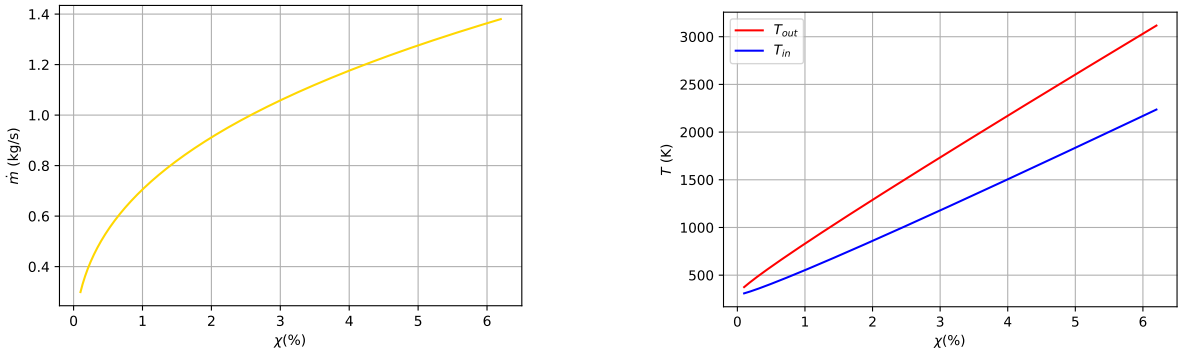

(a) Mass-flow rate as function of decay-heat fraction.

(b) In-/outlet temperature as function of decay-heat fraction.

Figure 4.1: Reference solutions for the mass-flow rate and the in-/outlet temperature as function of decay-heat fraction for air.

4.1.2. Altering the heat transfer coefficient

First the heat transfer coefficient h is altered, this is because of the fact that within the functions f and g the heat transfer coefficient not only exists linearly, but also exists within the exponential term in both equations. Because of the exponential, a small change in h will result in a relatively big change in the functions f and g. The heat transfer coefficient is altered from the reference value of 1.0×10^2 W/m^{2}K, up to 1.0×10^3 W/m^{2}K. The upper limit of 1.0×10^3 W/m^{2}K has been chosen to display the converging like behaviour of the relations shown in figure 4.2. Using these boundaries the values of $\dot{m}$, T_{in} and T_{out}, as function of h are determined. This results in the following relations:

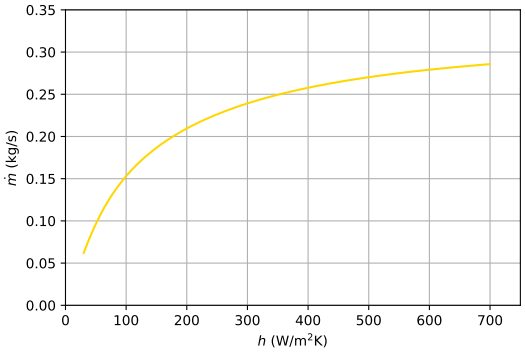

(a) Mass-flow rate as function of heat transfer coefficient.

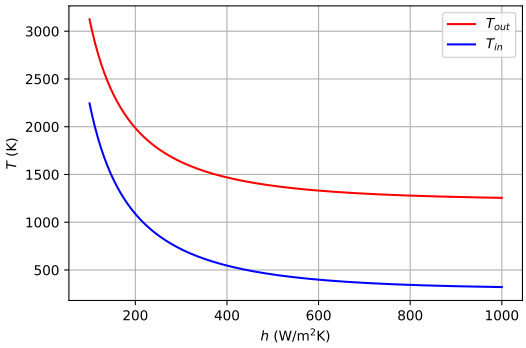

(b) In-/outlet temperature as function of heat transfer coefficient.

Figure 4.2: Solutions for the mass-flow rate and the in-/outlet temperature as function of the heat transfer coefficient for air.

In a more practical sense the heat transfer coefficient can be altered by changing the values of thermal conductivity k, the pipe diameter D and the average Nusselt number $\langle Nu \rangle$, as described in equation 2.27. Changing the type of fluid that flows through the heat-exchanger changes the value of k. The Nusselt number can at least be changed by changing the Reynolds, Rayleigh and Prandtl numbers. In order to change these numbers the properties which define them can be altered, these are mostly fluid properties.

4.1.3. Altering the heat exchanger length

Another non-linear parameter is the heat-exchanger length l. Looking at the model presented in figure 3.2 the value of l can only be changed into values for which $0 \leq l \leq H + a$ is true. If the heat-exchanger would cover the entire right leg its length would be a function of the chimney length as follows: $l(a) = H + a$. The chimney length a will be altered from the reference length 17 m, which is equivalent to: $l = 20$ m, up to 4.2×10^2 m, which is equivalent to: $l = 4.2 \times 10^2$ m [20] . Again the upper limit is chosen to display the converging like behaviour of the relations shown in figure 4.3:

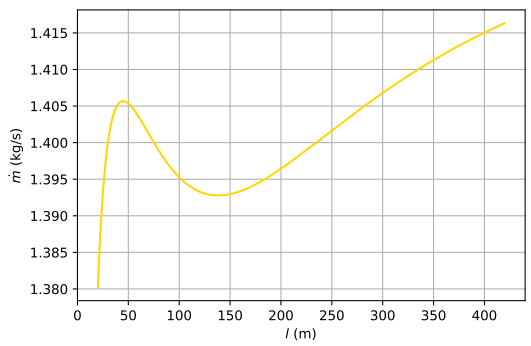

(a) Mass-flow rate as function of the heat-exchanger length.

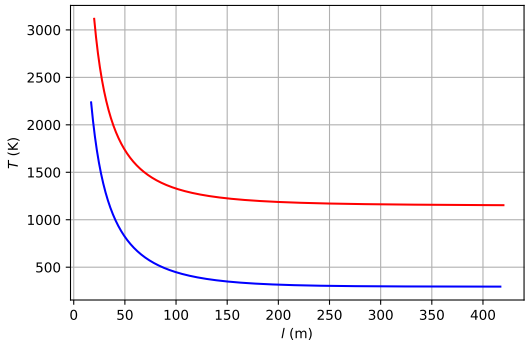

(b) In-/outlet temperature as function of the heat-exchanger length.

Figure 4.3: Solutions for the mass-flow rate and the in-/outlet temperature as function of the heat-exchanger length for air.

4.1.4. Altering the horizontal length

One of the parameters that only exists in a linear way within functions f and g is the horizontal length L. While all other parameter values remain unchanged, the value of L is altered from 3m up to 420m. The lower limit is the value which is used to evaluate the reference solution. The upper limit is chosen to be very large in order to see the complete relation L has to the mass-flow rate $\dot{m}$. How L relates to both $\dot{m}$ and T_{out} is displayed in figure 4.4:

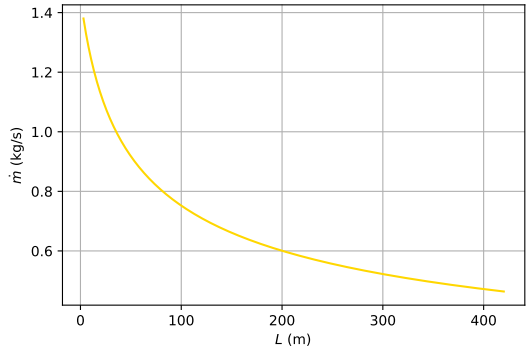

(a) Mass-flow rate as function of the horizontal length.

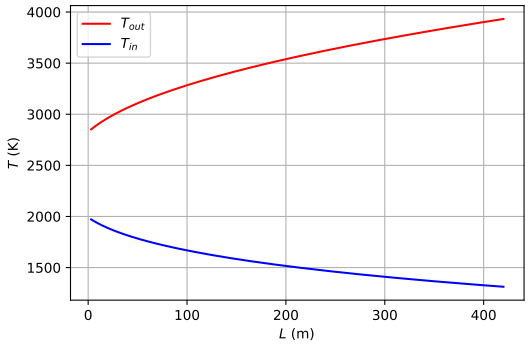

(b) In-/outlet temperature as function of the horizontal length.

Figure 4.4: Solutions for the mass-flow rate and the in-/outlet temperature as function of the horizontal length for air.

4.1.5. Altering the external temperature of the heat-exchanger

Another parameter that only exists in a linear way within functions f and g is the external heat-exchanger temperature $T_{\text{ext.}}$. While the other parameters remain fixed $T_{\text{ext.}}$ is altered from –10°C up to 30°C. These very large boundaries are chosen because they represent realistic temperature differences for the cooling fluid in the heat-exchanger. The behaviour of the solutions as function of $T_{\text{ext.}}$ are the following:

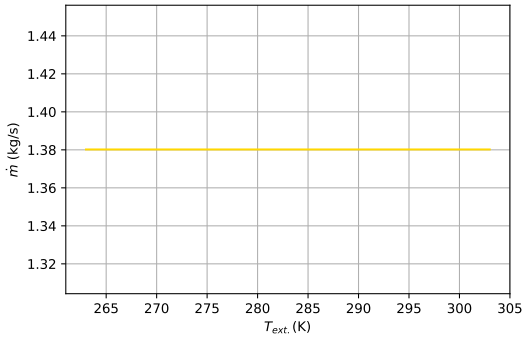

(a) Mass-flow rate as function of the external temperature.

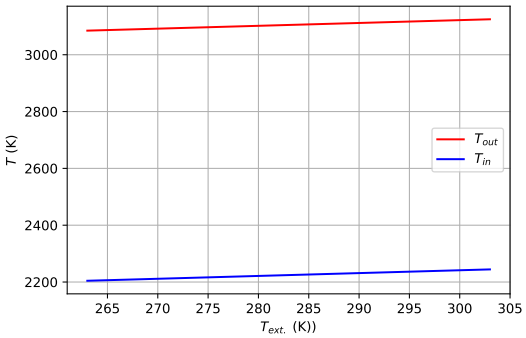

(b) In-/outlet temperature as function of the external temperature.

Figure 4.5: Solutions for the mass-flow rate and the in-/outlet temperature as function of the external temperature for air.

4.1.6. Altering the heat-exchanger length and the heat transfer coefficient

The heat transfer coefficient and heat-exchanger length are both of big influence to the values of $\dot{m}$ and T_{in}. Because of their influence a combination of these parameters was studied as well. The relation between parameters l, h and the solutions $\dot{m}$, T_{out} and T_{in} are given in figure 4.14:

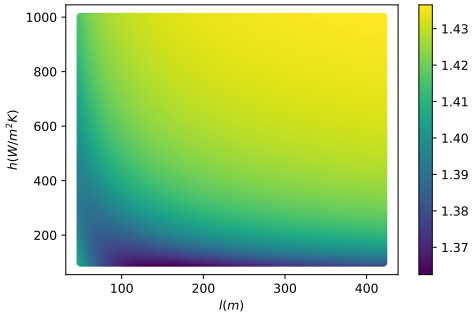

(a) Relation between the heat-exchanger length l (x-axis), the heat transfer coefficient h (y-axis) and the mass-flow rate $\dot{m}$ (color bar on the right in kg/s).

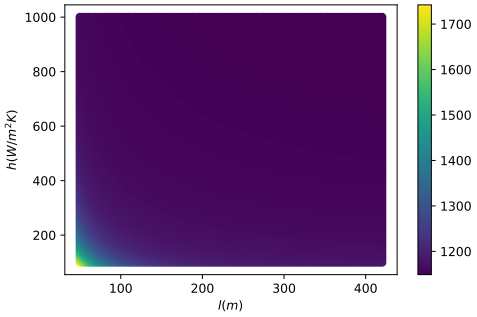

(b) Relation between the heat-exchanger length l (x-axis), the heat transfer coefficient h (y-axis) and the outlet temperature T_{out} (color bar on the right in K).

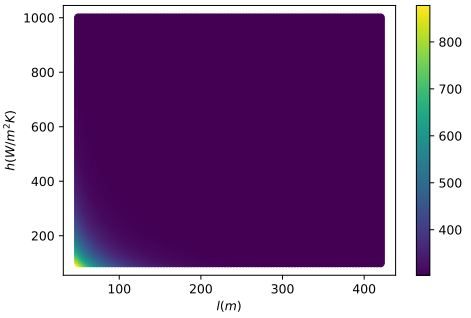

(c) Relation between the heat-exchanger length l (x-axis), the heat transfer coefficient h (y-axis) and the inlet temperature T_{in} (color bar on the right in K).

Figure 4.6: Solutions for the mass-flow rate, the outlet and the inlet temperature as function of heat-exchanger length and heat transfer coefficient for air.

The lower and upper limits of l and h are chosen the same as the limits used to evaluate the individual solutions.

4.2. Water cooled system

The second system that is studied is a system where water, rather than air, is used as a coolant. The properties are found at a reference temperature $T_0 = 20°\text{C}$ (293 K) and a pressure of 1 bar. Using this information the following physical properties [19] can be found:

Table 4.4: Physical constants water.

Constant	**Symbol**	**Unit**	
Reference temperature	T_0	K	293
Reference density	ρ_0	kg/m^3	1.0×10^3
Boiling point	T_b	K	3.7×10^2
Specific heat capacity	c_p	J/kgK	4.2×10^3
Thermal expansion coefficient	β	K^{-1}	0.21×10^{-3}
Dynamic viscosity	μ	Pas	1.0×10^{-3}

4.2.1. Reference solutions

The different parameters chosen for the reference solutions are presented in table 4.5. Furthermore, the decay-heat will be considered to be at its maximum value.

Table 4.5: Reference parameters water.

Parameters	**Symbol**	**Unit**	
Horizontal length	L	m	3
Chimney length	a	m	17
Heat Exchanger	l	m	20
Heat transfer coefficient	h	W/m^2K	3.0×10^3
External temperature	$T_{ext.}$	°C	20

The heat transfer coefficient of 3.0×10^3 W/m^2K is considered to be a minimum value for a water to air heat-exchanger [21]. The other reference parameters are chosen to be equal to those of the air cooled system. These choices result in the following reference solutions:

Table 4.6: Reference solutions water.

Variable	**Symbol**	**Unit**	
Mass-flow rate	$\dot{m}$	kg/s	29
Inlet temperature	T_{in}	K	1.1×10^3
Outlet temperature	T_{out}	K	1.1×10^3

Using the reference parameters, the reference solutions as function of the decay-heat fraction $\chi(t)$ can be determined, these are the following:

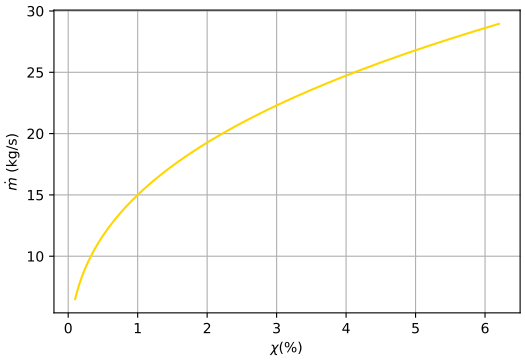

(a) Mass-flow rate as function of the decay-heat fraction.

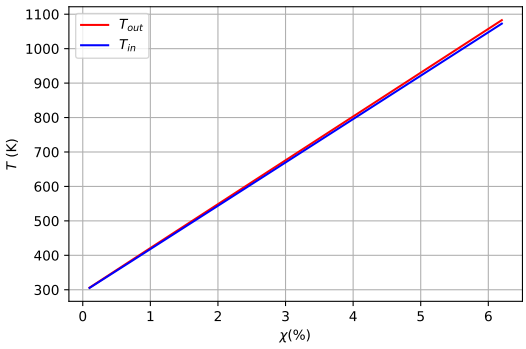

(b) In-/outlet temperature as function of decay-heat fraction.

Figure 4.7: Reference solutions for the mass-flow rate and the in-/outlet temperature as function of the decay-heat fraction for water.

4.2.2. Altering the heat transfer coefficient

Again the heat transfer coefficient h is altered first. This is for the same reason as the air cooled system. The heat transfer coefficient is altered from the reference value of 3.0×10^2 W/m^{2}K, up to 2.5×10^3 W/m^{2}K. The upper limit of 2.5×10^3 W/m^{2}K has been chosen because it represents a tubular system where coolant; water, is also cooled by water within the heat-exchanger [22]. Furthermore, the choice of the upper limit ensures that the converging like behaviour can be seen within figure 4.8. Using these boundaries, the values of $\dot{m}$, T_{out} and T_{out}, as function of h, are determined. This results in the following relations:

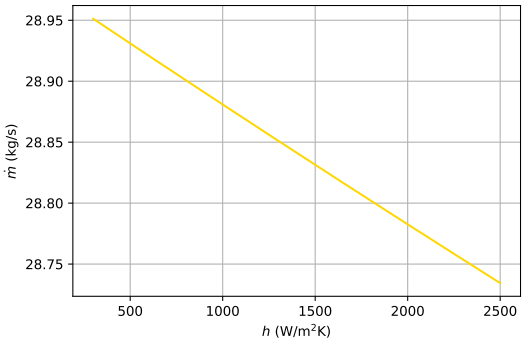

(a) Mass-flow rate as function of the heat transfer coefficient.

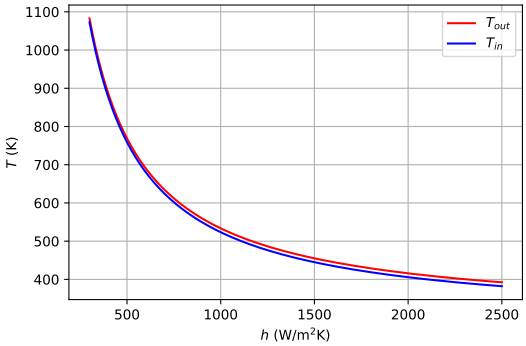

(b) In-/outlet temperature as function of the heat transfer coefficient.

Figure 4.8: Solutions for the mass-flow rate and the in-/outlet temperature as function of the heat transfer coefficient for water.

4.2.3. Altering the heat-exchanger length

The second parameter that will be altered is the heat-exchanger length l, this is yet again for the same reason as for the air cooled system. The limits are chosen to be the same as the air cooled system, and

for the same reasons. This results in the relations displayed in figure 4.9.

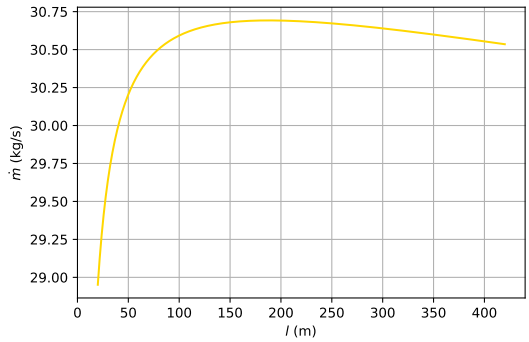

(a) Mass-flow rate as function of the heat-exchanger length.

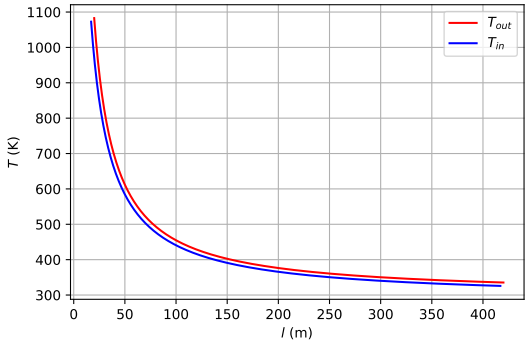

(b) In-/outlet temperature as function of the heat-exchanger length.

Figure 4.9: Solutions for the mass-flow rate and the in-/outlet temperature as function of the heat-exchanger length for water.

4.2.4. Altering the heat-exchanger length and the heat transfer coefficient

The studied parameters h and l are combined to study their collective contribution to the solutions $\dot{m}$, T_{out} and T_{in}. This results in the following relations:

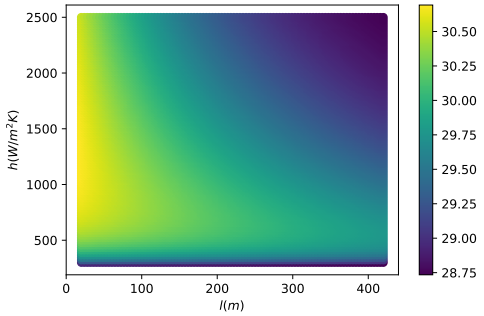

(a) Relation between the heat-exchanger length l (x-axis), the heat transfer coefficient h (y-axis) and the mass-flow rate $\dot{m}$ (color bar on the right in kg/s).

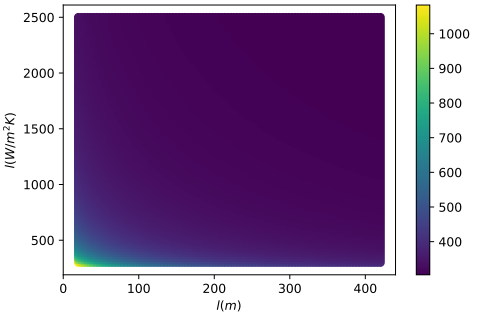

(b) Relation between the heat-exchanger length l (x-axis), the heat transfer coefficient h (y-axis) and the outlet temperature T_{out} (color bar on the right in K).

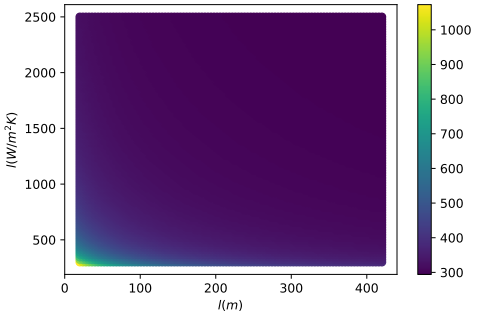

(c) Relation between the heat-exchanger length l (x-axis), the heat transfer coefficient h (y-axis) and the inlet temperature T_{in} (color bar on the right in K).

Figure 4.10: Solutions for the mass-flow rate, the outlet and the inlet temperature as function of heat-exchanger length and heat transfer coefficient for water.

The upper and lower limits are chosen for the same reason as described for the air cooled system.

4.3. Propyleneglycol cooled system

The third system that is studied is a system where Propyleneglycol is used as a coolant. The properties are found at a reference temperature $T_0 = 25°C$ (298 K) and a pressure of 1 bar. Using this information the following physical properties [23][24] can be found:

Table 4.7: Physical constants propyleneglycol.

Constant	**Symbol**	**Unit**	
Reference temperature	T_0	K	298
Reference density	ρ_0	kg/m^3	1.1×10^3
Boiling point	T_b	K	4.6×10^2
Specific heat capacity	c_p	J/kgK	2.5×10^3
Thermal expansion coefficient	β	K^{-1}	6.2×10^{-4}
Dynamic viscosity	μ	Pas	44×10^{-3}

4.3.1. Reference solutions

The different parameters chosen for the reference solutions are presented in table 4.8. Furthermore, the decay-heat will be considered to be at its maximum value.

Table 4.8: Reference parameters propyleneglycol.

Parameters	**Symbol**	**Unit**	
Horizontal length	L	m	3
Chimney length	a	m	17
Heat Exchanger	l	m	20
Heat transfer coefficient	h	W/m^2K	5.0×10^2
External temperature	$T_{ext.}$	°C	20

The heat transfer coefficient of 5.0×10^3 W/m^2K is considered [25] to be a minimum value for the overall heat transfer for a tube heat-exchanger. The other reference parameters are chosen to be equal to those of the air cooled system. These choices result in the following reference solutions:

Table 4.9: Reference solutions propyleneglycol.

Variable	**Symbol**	**Unit**	
Mass-flow rate	$\dot{m}$	kg/s	38
Inlet temperature	T_{in}	K	7.6×10^2
Outlet temperature	T_{out}	K	7.7×10^2

Using the reference parameters, the reference solutions as function of the decay-heat fraction $\chi(t)$ can be determined, these are the following:

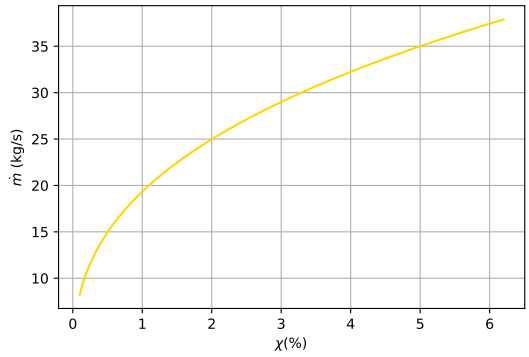

(a) Mass-flow rate as function of the decay-heat fraction.

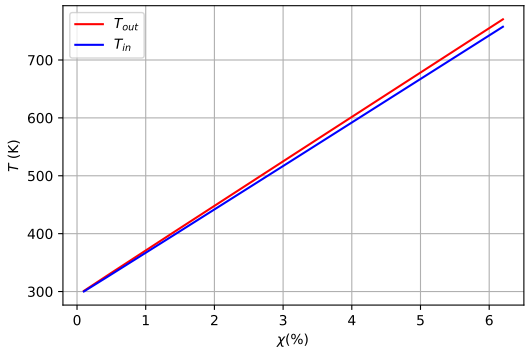

(b) In-/outlet temperature as function of decay-heat fraction.

Figure 4.11: Reference solutions for the mass-flow rate and the in-/outlet temperature as function of the decay-heat fraction for propyleneglycol.

4.3.2. Altering the heat transfer coefficient

The heat transfer coefficient is altered from the reference value of 5.0×10^2 W/m^{2}K, up to 2.0×10^3 W/m^{2}K. The upper limit of 2.0×10^3 W/m^{2}K is considered to be an upper limit for tubular convective heat transfer [25]. Using these boundaries, the values of $\dot{m}$, T_{out} and T_{out}, as function of h, are determined. This results in the following relations:

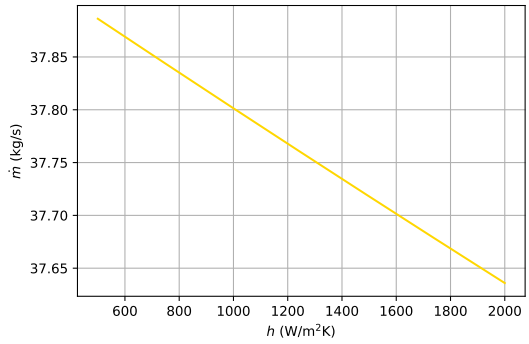

(a) Mass-flow rate as function of the heat transfer coefficient.

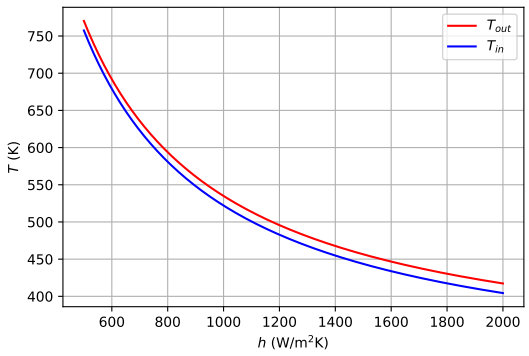

(b) In-/outlet temperature as function of the heat transfer coefficient.

Figure 4.12: Solutions for the mass-flow rate and the in-/outlet temperature as function of the heat transfer coefficient for propyleneglycol.

4.3.3. Altering the heat-exchanger length

The limits are chosen to be the same as the air/water cooled system, and for the same reasons. This results in the relations displayed in figure 4.13.

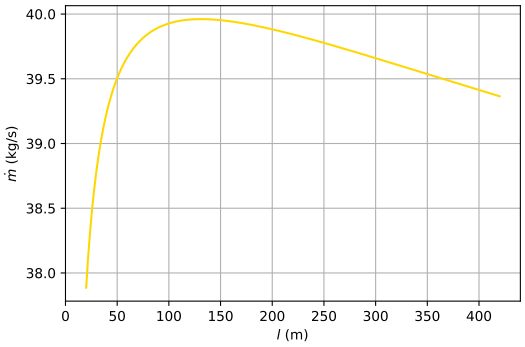

(a) Mass-flow rate as function of the heat-exchanger length.

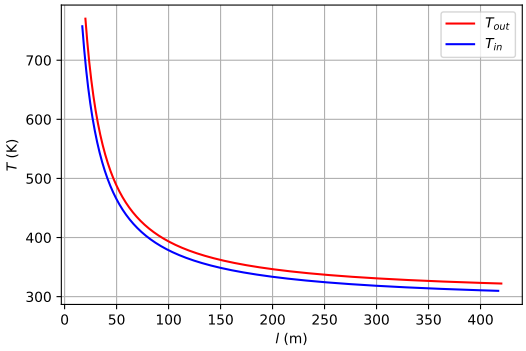

(b) In-/outlet temperature as function of the heat-exchanger length.

Figure 4.13: Solutions for the mass-flow rate and the in-/outlet temperature as function of the heat-exchanger length for propyleneglycol.

4.3.4. Altering the heat-exchanger length and the heat transfer coefficient

The studied parameters h and l are combined to study their collective contribution to the solutions $\dot{m}$, T_{out} and T_{in}. This results in the following relations:

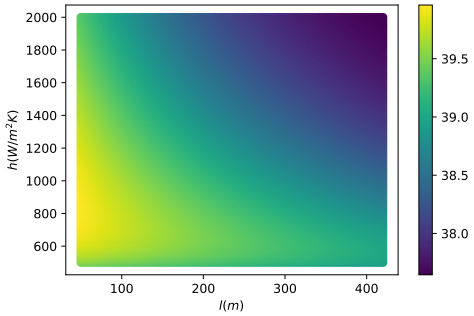

(a) Relation between the heat-exchanger length l (x-axis), the heat transfer coefficient h (y-axis) and the mass-flow rate $\dot{m}$ (color bar on the right in kg/s).

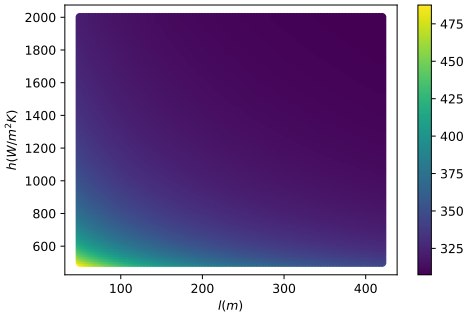

(b) Relation between the heat-exchanger length l (x-axis), the heat transfer coefficient h (y-axis) and the outlet temperature T_{out} (color bar on the right in K).

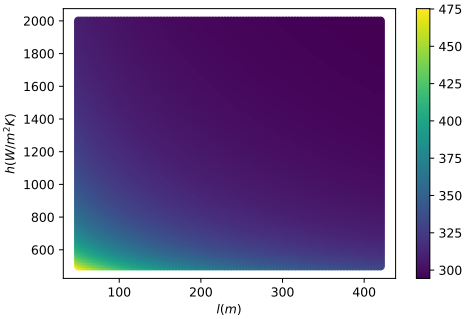

(c) Relation between the heat-exchanger length l (x-axis), the heat transfer coefficient h (y-axis) and the inlet temperature T_{in} (color bar on the right in K).

Figure 4.14: Solutions for the mass-flow rate, the outlet and the inlet temperature as function of heat-exchanger length and heat transfer coefficient for propyleneglycol.

The upper and lower limits are chosen for the same reason as described for the air/water cooled system.

4.4. Carbon dioxide cooled system

The fourth system that is studied is a system where carbon dioxide is used as a coolant. The properties are found at a reference temperature $T_0 = 25°C$ (298 K) and a pressure of 1 bar. Using this information the following physical properties [19] can be found:

Table 4.10: Physical constants carbon dioxide.

Constant	**Symbol**	**Unit**	
Reference temperature	T_0	K	298
Reference density	ρ_0	kg/m^3	1.8
Specific heat capacity	c_p	J/kgK	0.85×10^3
Thermal expansion coefficient	β	K^{-1}	45×10^{-4}
Dynamic viscosity	μ	Pas	15×10^{-6}

4.4.1. Reference solutions

The different parameters are chosen to be the same as those for air, and are presented in table 4.11

Table 4.11: Reference parameters carbon dioxide.

Parameters	**Symbol**	**Unit**	
Horizontal length	L	m	3
Chimney length	a	m	17
Heat Exchanger	l	m	20
Heat transfer coefficient	h	W/m^2K	1.0×10^2
External temperature	$T_{ext.}$	°C	20

These choices result in the following reference solutions:

Table 4.12: Reference solutions carbon dioxide.

Variable	**Symbol**	**Unit**	
Mass-flow rate	$\dot{m}$	kg/s	2,2
Inlet temperature	T_{in}	K	2.2×10^3
Outlet temperature	T_{out}	K	3.0×10^3

Using the reference parameters, the reference solutions as function of the decay-heat fraction $\chi(t)$ can be determined, these are the following:

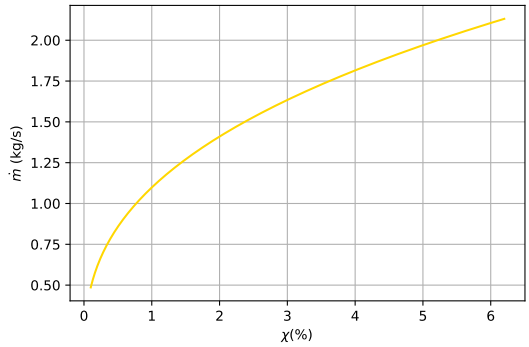

(a) Mass-flow rate as function of the decay-heat fraction.

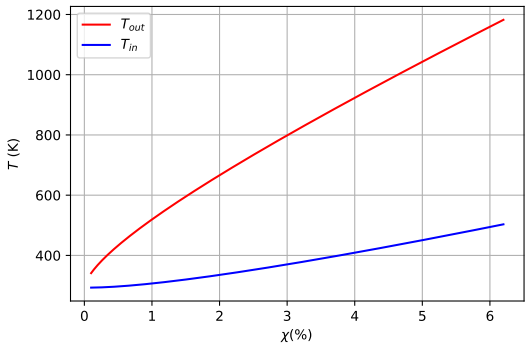

(b) In-/outlet temperature as function of decay-heat fraction.

Figure 4.15: Reference solutions for the mass-flow rate and the in-/outlet temperature as function of the decay-heat fraction for carbon dioxide.

4.4.2. Altering the heat transfer coefficient

The heat transfer coefficient is altered from the reference value of 1.0×10^2 W/m^{2}K, up to 1.0×10^3 W/m^{2}K, the same as the air cooled system. Using these boundaries, the values of $\dot{m}$, T_{out} and T_{out}, as function of h, are determined. This results in the following relations:

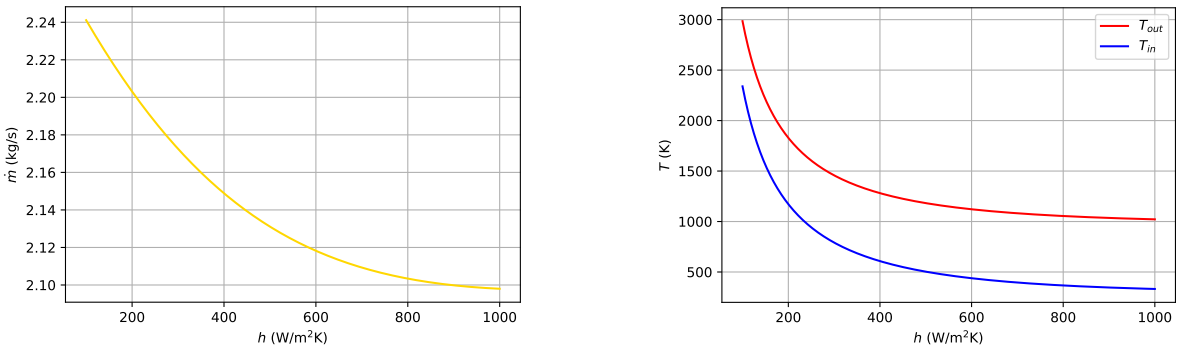

(a) Mass-flow rate as function of the heat transfer coefficient.

(b) In-/outlet temperature as function of the heat transfer coefficient.

Figure 4.16: Solutions for the mass-flow rate and the in-/outlet temperature as function of the heat transfer coefficient for carbon dioxide.

4.4.3. Altering the heat-exchanger length

The limits are chosen to be the same as the air/water cooled system, and for the same reasons. This results in the relations displayed in figure 4.17.

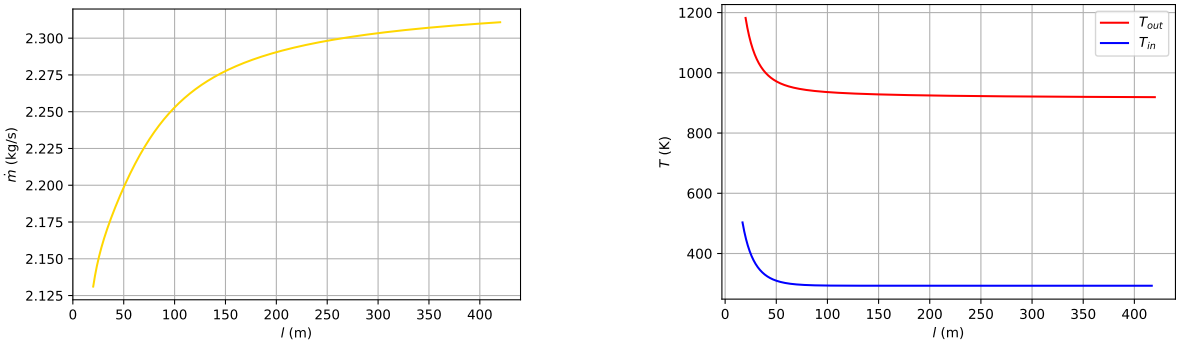

(a) Mass-flow rate as function of the heat-exchanger length.

(b) In-/outlet temperature as function of the heat-exchanger length.

Figure 4.17: Solutions for the mass-flow rate and the in-/outlet temperature as function of the heat-exchanger length for carbon dioxide.

4.4.4. Altering the heat-exchanger length and the heat transfer coefficient

The studied parameters h and l are combined to study their collective contribution to the solutions $\dot{m}$, T_{out} and T_{in}. This results in the following relations:

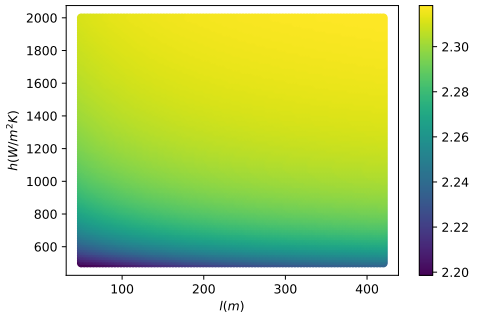

(a) Relation between the heat-exchanger length l (x-axis), the heat transfer coefficient h (y-axis) and the mass-flow rate $\dot{m}$ (color bar on the right in kg/s).

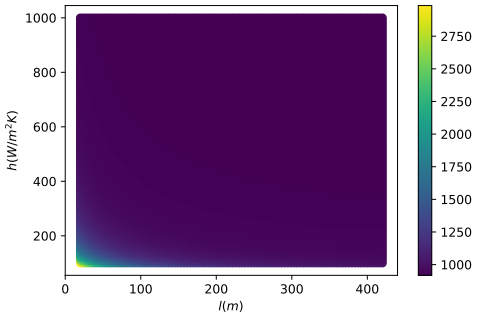

(b) Relation between the heat-exchanger length l (x-axis), the heat transfer coefficient h (y-axis) and the outlet temperature T_{out} (color bar on the right in K).

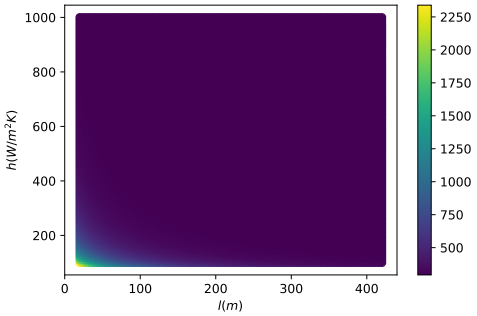

(c) Relation between the heat-exchanger length l (x-axis), the heat transfer coefficient h (y-axis) and the inlet temperature T_{in} (color bar on the right in K).

Figure 4.18: Solutions for the mass-flow rate, the outlet and the inlet temperature as function of heat-exchanger length and heat transfer coefficient for carbon dioxide.

The upper and lower limits are chosen for the same reason as described for the air/water cooled system.

5

Discussion

The results, which are given in chapter 4, are determined using the functions f and g. When a set of parameter values are chosen, the solutions of these functions are the mass-flow rate $\dot{m}$ and inlet temperature T_{in}, the outlet temperature is determined using T_{in}. By altering the different parameters in value and type, and by changing the type of coolant, the behaviour of the mass-flow rate and outlet temperature was studied with respect to these choices. Good solutions for functions f and g should ensure that both functions are approximately zero, when filled back into functions f and g. To display the trustworthiness of the solutions: $\dot{m}_{\text{sol}}$ and $\dot{T}_{\text{in}}$, the solutions are filled back into functions f and g for all the situations presented in chapter 4. This leads to the absolute error functions presented in appendix D.

Most errors are in the order of 10^{-6}, or lower. These errors are very small in comparison to the order of magnitude of the solutions for the mass-flow rate and inlet temperature, which are in the order of 10^{-1} up to 10^{1}, and 10^{2} up to 10^{3} receptively. Local error peaks that are bigger than 10^{-6}, as well as the local error peak that are smaller, can be explained by the fact that in the `scipy.optimize.fsolve` routine the initial guesses the same for all parameter values by making use of a `for loop`, as shown in appendix B. More accurate solutions would probably follow if the algorithm had more accurate initial guesses. The initial guesses that are used to generate the results, presented in chapter 4, are chosen because they give relatively 'good' solutions for the different parameter values. The initial guess forms an average initial guess for all the solutions, choosing a local initial guess that iterates inside the `for loop` would solve this problem. The solutions for the external temperature for the air cooled system are very large in comparison to other errors. The f function shows very large errors within the entire defined parameter space. Because of the fact that this behaviour is unique for this particular parameter, and function, it is hard to gain insight into the precise nature of these errors.

First of all it is noticed that the mass-flow behaves more or less like a square root function for increasing decay-heat fractions. The in-/outlet temperatures decrease linearly as function of the decay-heat fraction. The air cooled system shows very high values for the outlet temperature, the lowest value is approximately 1.2×10^{3} K. The inlet temperatures are lower, the lowest value is approximately 3.0×10^{2} K. The in-/outlet temperatures are most sensitive for the heat transfer coefficient and heat-exchanger length. The temperatures do however converge to values that are more or less of constant value. Choosing values for the heat transfer coefficient that are bigger than approximately 6.0×10^{2} W/m^{2}K result in no notable effect for the in-/outlet temperature. The increase of the mass-flow rate is most sensitive for the heat transfer coefficient, an increasing heat-transfer coefficient results in the increase of the mass-flow rate. The mass-flow rate also converges to a more and more constant value, the further increase of the heat transfer coefficient results in no notable change in the mass-flow rate. Changing the horizontal length and external temperature results in no desirable change for the mass-flow rate and in-/outlet temperature. Altering both the heat transfer coefficient and the heat-exchanger length at the same time results in maximum mass-flow rates up to 1.4 kg/s for high values of these parameters: $h > 5.0 \times 10^{2}$ W/m^{2}K, $l > 1.5 \times 10^{2}$ m. The in-/outlet temperatures decrease very fast, to 3.5×10^{2}K and

1.3×10^3 K respectively.

For the water cooled system the mass-flow rate slightly decreases for increasing heat transfer coefficient. The decrease however, is very small (2.0×10^{-1} kg/s) with respect to the values of the mass-flow rate (that are in the order of 2.9×10^1 kg/s). It can therefore be concluded that there is no notable or desired effect for the mass-flow rate as function of the heat transfer coefficient. The in-/outlet temperatures decrease fast as function of the heat transfer coefficient, the slope does however flat out for higher heat transfer coefficients: $h > 1.5 \times 10^3$ W/m^{2}K. The mass-flow shows more notable effects as function of the heat-exchanger length. The mass-flow rate keeps increasing for values up to $l = 1.5 \times 10^3$ m after which it starts decreasing. The increase of the mass-flow rate as function of the heat exchanger length (2.0 kg/s) is more notable than the increase seen for the heat transfer coefficient. The in-/outlet temperatures decrease very fast as function of the heat-exchanger length. For higher values of the heat exchanger length ($l > 2.5 \times 10^2$ m) the temperatures will converge towards a more or less constant of value (approximately 3.5×10^2 K). Increasing the value of heat-exchanger length beyond $l = 2.5 \times 10^2$ m results in no notable change in temperature. Altering the heat transfer coefficient and the heat-exchanger length together, results in maximum values for the mass-flow (up to 31 kg/s rate for: $l \leq 1.0 \times 10^2$ m and heat transfer coefficients between $(1.0 \times 10^3 - 1.5 \times 10^3)$ W/m^{2}K. The in-/outlet temperature decreases very fast towards approximately 4.0×10^2 K.

The propyleneglycol cooled system shows very similar behaviour in comparison to the water cooled system. The decrease in mass-flow rate as function of the heat transfer coefficient is not notable (2.0×10^{-1} kg/s for mass-flow rates in the order of 3.8×10^1 kg/s). The temperatures however, are significantly lower as function of the heat transfer coefficient. Furthermore, it is noticed that the functions have a less strong converging shape. The mass-flow rate increases as function of the heat-exchanger length for values up to 1.0×10^2 m after which it starts decreasing. The behavior of the in-/outlet temperatures is very similar to the water cooled system but the temperatures are significantly lower. The combination of both parameters results in mass-flow rates up to 40 kg/s for $l \leq 1.0 \times 10^1$ m and $h = (6.0 \times 10^2 - 1.2 \times 10^3)$ W/m^{2}K. The in-/outlet temperatures decreases very fast towards approximately 4.0×10^2 K.

The carbon dioxide cooled system shows very similar behaviour in comparison to the air cooled system. For the heat transfer coefficient it is notable that the mass-flow rate decreases. The in-/outlet temperature converges to a lower value (approximately 2.0×10^2 K and 1.0×10^3 K respectively) in comparison to the air cooled system. As function of the heat exchanger length the mass-flow rate increases slightly. The temperatures decrease very fast towards approximately 1.0×1.0^2 K and 1.0×10^3 K respectively. The combination of both parameters shows increasing mass-flow rate values up to 2.3 kg/s for $h \geq 3.0 \times 10^3$ W/m^{2}K. The in-/outlet temperatures converge very fast towards approximately 3.5×10^2 K.

6

Conclusions

6.1. Concluding remarks

The closed loop cooling cycle was constructed in order to find a more adequate cooling system for the EDT of a molten salt reactor. The EDT is cooled by a coolant that flows through the cooling cycle a coolant flows Analytical steady state solutions for the mass-flow rate and the in-/outlet temperature were determined using an algorithm. By making use of the algorithm, the effect of different loop parameters and coolants was studied. Desirable solutions are those which ensure a high mass-flow rate and low in-/outlet temperatures. The generated results give insight in the relationship between these solutions and the heat transfer coefficient, the heat-exchanger length, the horizontal loop length and the external temperature for different coolants.

For the decay-heat fraction is found that the mass-flow rates increases like a square root function while the in-/outlet temperatures increase linearly for decay-heat fractions. Furthermore, the horizontal length and the external temperature both show no notable or desirable effect on the mass-flow rate and the in-/outlet temperature. The maximum mass-flow rate for the air cooled system is: 1.4 kg/s for $h > 5.0 \times 10^2$ W/m^{2}K, $l > 1.5 \times 10^2$ m, the water cooled system has a maximum mass-flow rate of 31 kg/s for $l \leq 1.0 \times 10^2$ m, $h = (1.0 \times 10^3 - 1.5 \times 10^3)$ W/m^{2}K, the propyleneglycol cooled system shows a maximum mass-flow rate of 40 kg/s for $l \leq 1.0 \times 10^1$ m and $h = (6.0 \times 10^2 - 1.2 \times 10^3)$ W/m^{2}K and for the carbon dioxide shows a maximum mass-flow rate of 2.3 kg/s for $h \geq 3.0 \times 10^3$ W/m^{2}K. The in-/outlet temperature for air: 3.5×10^2K and 1.3×10^3 K respectively, water: 4.0×10^2 K, propyleneglycol: 4.0×10^2 K and carbon dioxide: 5.0×10^2 K 1.0×10^3 K. The propyleneglycol shows the most desirable solutions, it has the highest mass-flow rate and the lowest temperatures of the investigated coolants. Water also has a desirable set of solutions with a high mass-flow rate and low temperatures. Carbon dioxide shows desirable solutions in terms of the temperatures, but less desirable solutions for the mass-flow rate. The mass-flow rate of air is the lowest of the four investigated coolants. The air temperatures are highest in comparison to the other coolants. Furthermore, it is noticed that the parameters concerning the heat-exchanger: the heat-transfer coefficient and the heat-exchanger length are of the biggest influence in the proposed loop model.

6.2. Recommendations

The discussed closed loop cooling cycle forms an analytical basis for further investigation. Within the current investigation multiple simplifications have been made in order to gain analytical solutions. The heat production term in the EDT has been chosen to be independent of the height of the EDT. A more realistic model takes into account that the heat-flux will decrease as function of the height because of the increasing coolant temperature in the EDT. Furthermore, the friction factor and heat transfer coefficients have been estimated by looking at similar geometries and systems. By making use of more advanced physical simulations the solutions will become more realistic. The analytical model could form a mathematical basis for these simulations. In the model the altered parameters are not the only values that can be changed. The values of the EDT height, the pipe diameter and/or the cell geometry

can be changed as well. A parameter that could be investigated in a different way than shown in the current investigation is the chimney height. The heat-exchanger length has been chosen to be the same as the total height of closed loop, to create more buoyancy the exchanger could be placed as high as possible (relative to the bottom of the EDT). Lastly, the effect of other coolants can be studied: gasses under pressure or other type of cooling liquids.

Bibliography

[1] Charles Forsberg. Molten salt reactors (msrs), 2002.

[2] E MERL. Molten salt reactor workshop -psi - concept of molten salt fast reactor concept of molten salt fast reactor, 2017.

[3] Mattia Massone, Shisheng Wang, and Andrei Rineiski. Group: Transmutation analytical modeling of the emergency draining tank for a molten salt reactor, 09 2018.

[4] Jan Leen Kloosterman and Danny Lathouwers. Kick-off meeting bep, 09 2022.

[5] Shisheng Wang, Mattia Massone, Andrei Rineiski, and E Merle-Lucotte. Analytical investigation of the draining system for a molten salt fast reactor, 2016.

[6] Jan-Leen Kloosterman. Thorium in msr, 04 2022.

[7] H Koopman. Development of the stealth-code and investigation of the effects of feedwater sparger positioning on the thermal-hydraulic stability of natural circulation boiling water reactors, 06 2008.

[8] Joseph Boussinesq and University of California Libraries. *Théorie de l'écoulement tourbillonnant et tumultueux des liquides dans les lits rectilignes a grande section.* Paris, Gauthier-Villars et fils, 1897.

[9] Robert Alexander Adams, Christopher Essex, and Pearson. *Calculus : a complete course.* Pearson, Copyright, 2014.

[10] M. Zarei. An approach to the coupled dynamics of small lead cooled fast reactors. *Nuclear Engineering and Technology*, 51:1272–1278, 08 2019.

[11] Michael J Moran, Howard N Shapiro, Daisie D Boettner, Margaret B Bailey, and John Wiley. *Moran's principles of engineering thermodynamics.* Wiley, 2018.

[12] Harrie Akker and Robert Frank Mudde. *Fysische transportverschijnselen.* TU Delft Press, 2014.

[13] Barhm Abdullah Mohamad. Free and forced convection. 2022.

[14] E. Sanvicente, S. Giroux-Julien, C. Ménézo, and H. Bouia. Transitional natural convection flow and heat transfer in an open channel. *International Journal of Thermal Sciences*, 63:87104, 01 2013.

[15] Magnus J. Wenninger. *Polyhedron Models.* Cambridge University Press, 04 1974.

[16] G E Klinzing, F Rizk, R Marcus, L S Leung, and Springerlink (Online Service. *Pneumatic Conveying of Solids : A theoretical and practical approach.* Springer Netherlands, 2010.

[17] SciPi community. scipy.optimize.fsolve scipy v1.9.3 manual, 2022.

[18] Moré J J, Garbow B S, and Hillstrom K E. User guide for minpack-1, 08 1980.

[19] M Janssen and M. M. C. G. Warmoeskerken. *Transport Phenomena Data Companion.* Hodder Education, third edition, 2006.

[20] Guinness World Records. Tallest chimney, 2022.

[21] John M Coulson and Raymond K Sinnott. *Chemical engineering / 6, Chemical engineering design.*, volume 6. Pergamon Pr, second edition, 1993.

[22] Alfa Level. The theory behind heat transfer plate heat exchangers, 2022.

[23] Carpemar. Propylene glycol industrial grade, 09 2016.

[24] Cameo Chemicals. Propylene glycol ppg cautionary response information common synonyms thick liquid colorless odorless mixes with water, 1999.

[25] Uschuas Dipta Das, Moham Ed Abdur Razzaq, M. K. Sajib, and J. U. Ahamed. Heat transfer analysis of propylene glycol and water mixture based tio2 nanofluids in a shell and tube heat exchanger. *International Conference on Mechanical Engineering and Renewable Energy 2019*, 12 2019.

A

Buoyancy - Friction

Friction term

$$\oint_s g(\rho_0 A)^2\left[1-\beta(T-T_0)\right](\hat{z}\cdot\hat{s})ds = g(\rho_0 A)^2\left[I_1+I_2+I_3+I_4+I_5\right] \\ = \oint_s \frac{-f\dot{m}_s^2}{2D_\mathrm{h}}ds = \left[\frac{-f\dot{m}_s^2}{2D_\mathrm{h}}s\right]_0^{2(H+a+L)} = \frac{-f\dot{m}_s^2}{D_\mathrm{h}}(H+a+L) \tag{A.1}$$

Buoyancy term

$$I_1 = \int_0^H \left[1-\beta\Big(\frac{q'_{\mathrm{th.}}}{\dot{m}_s c_\mathrm{p}}s+T_\mathrm{in}-T_0\Big)\right](\hat{z}\cdot\hat{s})ds = \int_0^H \left[1-\beta\Big(\frac{q'_{\mathrm{th.}}}{\dot{m}_s c_\mathrm{p}}s+(T_\mathrm{in}-T_0)\Big)\right](1)ds \\ = s\Big[1-\beta\Big(0.5\frac{q'_{\mathrm{th.}}}{\dot{m}_s c_\mathrm{p}}s+(T_\mathrm{in}-T_0)\Big)\Big]_0^H = H\Big[1-\beta\Big(0.5\frac{q'_{\mathrm{th.}}}{\dot{m}_s c_\mathrm{p}}H+(T_\mathrm{in}-T_0)\Big)\Big] \tag{A.2}$$

$$I_2 = \int_H^{H+a}\left[1-\beta(T_\mathrm{out}-T_0)\right](\hat{z}\cdot\hat{s})ds = \int_H^{H+L}\left[1-\beta(T_\mathrm{out}-T_0)\right](1)\ ds \\ = s\Big[1-\beta(T_\mathrm{out}-T_0)\Big]_H^{H+a} = a\big[1-\beta(T_\mathrm{out}-T_0)\big] = a\Big[1-\beta\Big(\frac{q'_{\mathrm{th.}}}{\dot{m}_s c_\mathrm{p}}H+(T_\mathrm{in}-T_0)\Big)\Big] \tag{A.3}$$

$$I_3 = \int_H^{H+L}\left[1-\beta(T_\mathrm{out}-T_0)\right](\hat{z}\cdot\hat{s})ds = \int_H^{H+L}\left[1-\beta(T_\mathrm{out}-T_0)\right](0)\ ds = 0 \tag{A.4}$$

$$I_4 = \int_{H+a+L}^{H+a+L+l} \Big[1-\beta\Big(T_{\text{ext.}} + (T_{\text{out}} - T_{\text{ext.}}) \exp\Big[\frac{hD}{\dot{m}_s c_{\text{p}}}(H+L)\Big] \exp\Big[\frac{-hD}{\dot{m}_s c_{\text{p}}} s\Big] - T_0\Big)\Big](\hat{z}\cdot\hat{s})\,ds$$

$$= \int_{H+a+L}^{H+a+L+l} \Big[1-\beta\Big(T_{\text{ext.}} + (T_{\text{out}} - T_{\text{ext.}}) \exp\Big[\frac{hD}{\dot{m}_s c_{\text{p}}}(H+L)\Big] \exp\Big[\frac{-hD}{\dot{m}_s c_{\text{p}}} s\Big] - T_0\Big)\Big](-1)\;\; ds$$

$$= -\Big[s\big[1-\beta(T_{\text{ext.}} - T_0)\big] - \beta(T_{\text{out}} - T_{\text{ext.}}) \exp\Big[\frac{hD}{\dot{m}_s c_{\text{p}}}(H+L)\Big] \exp\Big[\frac{-hD}{\dot{m}_s c_{\text{p}}} s\Big] \frac{-\dot{m}_s c_{\text{p}}}{hD}\Big]_{H+a+L}^{H+a+L+l} \tag{A.5}$$

$$= -l\big[1-\beta(T_{\text{ext.}} - T_0)\big] + \beta(T_{\text{out}} - T_{\text{ext.}})\Big(1-\exp\Big[\frac{-hD}{\dot{m}_s c_{\text{p}}} l\Big]\Big)\frac{\dot{m}_s c_{\text{p}}}{hD}$$
$$= -l\big[1-\beta(T_{\text{ext.}} - T_0)\big] + \beta\Big(\frac{q'_{\text{th.}}}{\dot{m}_s c_{\text{p}}} + (T_{\text{in}} - T_{\text{ext.}})\Big)\Big(1-\exp\Big[\frac{-hD}{\dot{m}_s c_{\text{p}}} l\Big]\Big)\frac{\dot{m}_s c_{\text{p}}}{hD}$$

$$I_5 = \int_{H+a+L+l}^{2(H+a)+L} \big[1-\beta(T_{\text{in}} - T_0)\big](\hat{z}\cdot\hat{s})\,ds = \int_{H+a+L+l}^{2(H+a)+L} \big[1-\beta(T_{\text{in}} - T_0)\big](-1)\,ds$$
$$= -\Big[1-\beta(T_{\text{in}} - T0)\Big]_{H+a+L+l}^{2(H+a)+L} = \big[1-\beta(T_{\text{in}} - T_0)\big](l-H-a) \tag{A.6}$$

$$I_6 = \int_{2(H+a)+L}^{2(H+a+L)} \big[1-\beta(T - T_0)\big](\hat{z}\cdot\hat{s})\,ds = \int_{2(H+a)+L}^{2(H+a+L)} \big[1-\beta(T_{\text{in}} - T_0)\big](0)\,ds = 0 \tag{A.7}$$

The Buoyancy - friction relation

$$-f\frac{\dot{m}_s^2}{DA\rho_0}(H+a+L) = H\Big[1-\beta\Big(0.5\frac{q'_{\text{th.}}}{\dot{m}_s\langle c_{\text{p}}\rangle}H + (T_{\text{in}} - T_0)\Big)\Big] + a\Big[1-\beta\Big(\frac{q'_{\text{th.}}}{\dot{m}_s\langle c_{\text{p}}\rangle}H + (T_{\text{in}} - T_0)\Big)\Big] -$$
$$l\big[1-\beta(T_{\text{ext.}} - T_0)\big] + \beta\Big(\frac{q'_{\text{th.}}}{\dot{m}_s\langle c_{\text{p}}\rangle} + (T_{\text{in}} - T_{\text{ext.}})\Big)\Big(1-\exp\Big[\frac{-hD}{\dot{m}_s\langle c_{\text{p}}\rangle} l\Big]\Big)\frac{\dot{m}_s\langle c_{\text{p}}\rangle}{hD} + \tag{A.8}$$
$$\big[1-\beta(T_{\text{in}} - T_0)\big](l-H-a)$$

B

Code

Presented functions to algorithm

```
def func(x): # Darcy friction factor

    Re = x[0] * D_h / (mu * A) # Reynolds number

    f = 4 * (0.0014 + 0.125 * Re**(-0.32)) # friction factor

    I1 = H * (1 - beta * (0.5 * q / (x[0] * cp_0) * H + (x[1] - T0)))  # m

    I2 = a * (1 - beta * (q / (x[0] * cp_0) * H + (x[1] - T0)))  # m

    I3 = 0  # m

    I4 = -l * (1 - beta * (T_ext - T0)) +
    beta * (q / (x[0] * cp_0) + (x[1] - T_ext)) *
    (1 - np.exp(-h * D / (x[0] * cp_0) * l)) * x[0] * cp_0 / (h * D) # m

    I5 = (1 - beta * (x[1] - T0)) * (l - H - a)  # m

    I6 = 0  # m
```

```
    Friction = -f * x[0]**2 * (H + a + L) / D_h  # m


    f = g * (rho_0 * A)**2 * (I1 + I2 + I3 + I4 + I5 + I6) - Friction

    g = (x[1] - T_ext) - (H * q / (x[0] * cp_0) + x[1] - T_ext) *
                                 np.exp(-h * D / (x[0] * cp_0) * l)


    return [f, g] # x[0] = dot{m}, x[1] = T_in
```

Example code for solutions as functions of decay-heat fraction

```
M_sol = np.zeros(len(decay_heat_fraction))
T_in_sol = np.zeros(len(decay_heat_fraction))
T_out_sol = np.zeros(len(decay_heat_fraction))
f_check = np.zeros(len(decay_heat_fraction))
g_check = np.zeros(len(decay_heat_fraction))


for i in range(0, len(decay_heat_fraction)):


    q = Q_0[i]
    a = 17
    H = 3
    L = 3
    l = H + a
    h = 500

    M_sol[i], T_in_sol[i] = fsolve(func, x0=[1e-2, 1e4],
    factor=0.1,
    xtol=1e-11)
    T_out_sol[i] = T_in_sol[i] + H * q / (M_sol[i] * cp_0)

    f_check[i], g_check[i] = np.abs(func([M_sol[i], T_in_sol[i]]))
```

C

EDT data

Constant [4]	**Symbol**	**Unit**	
Total fuel-salt volume	$V_{\text{tot.}}$	m^3	18
Inner fuel-salt radius	R_4	m	37×10^{-2}
Outer fuel-salt radius	R_5	m	39×10^{-2}
Nominal power	$Q_{\text{tot.}}$	W	3.0×10^9
Pipe radius	R_1	m	13×10^{-2}
EDT height	H	m	3.0

D

Absolute error functions

D.1. Air cooled system

Decay-heat fraction

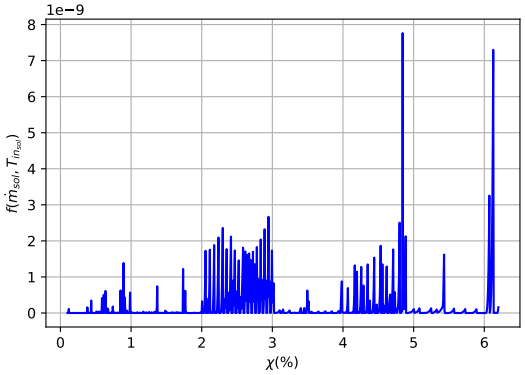

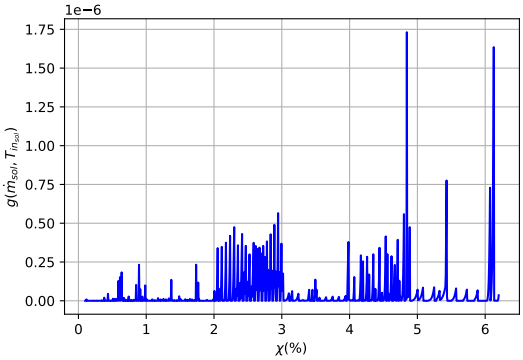

Heat transfer coefficient

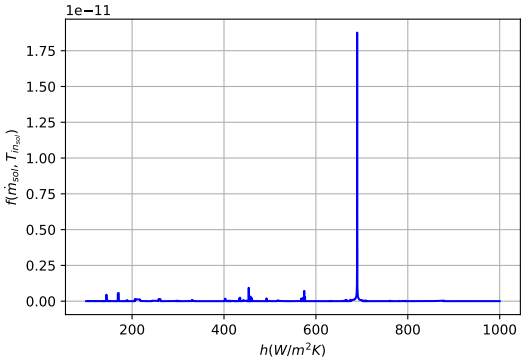

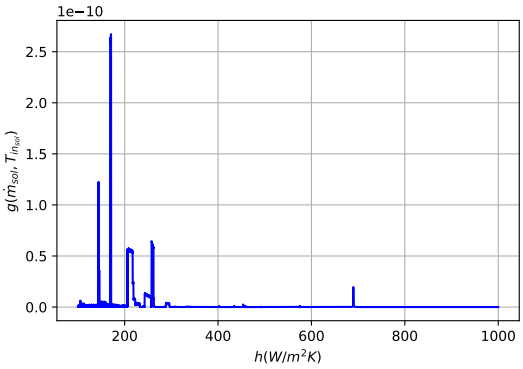

Heat-exchanger length

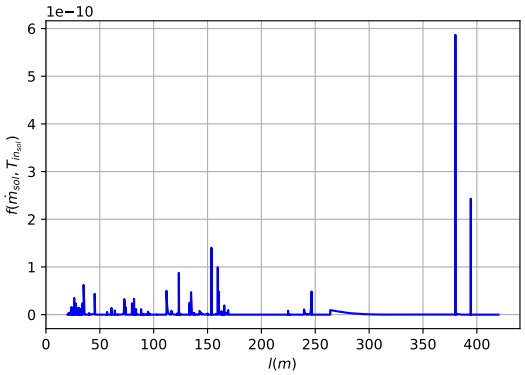

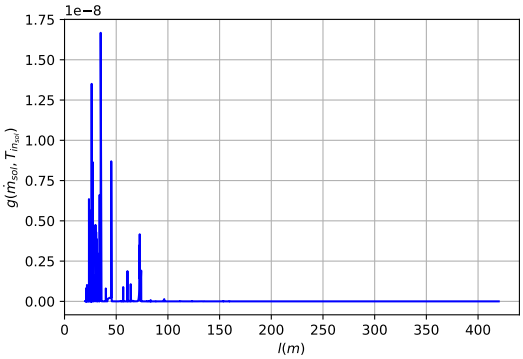

Horizontal length

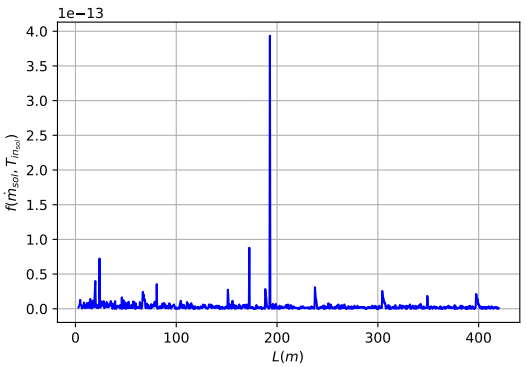

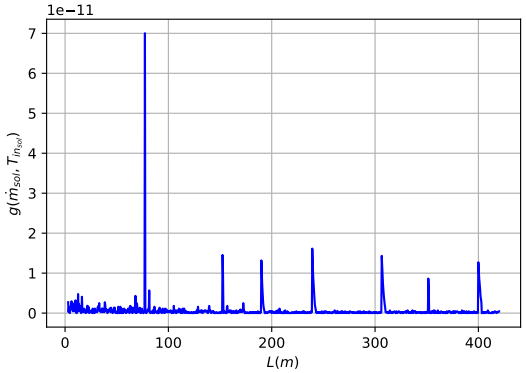

External temperature

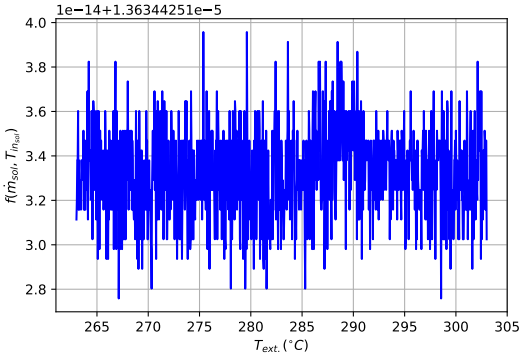

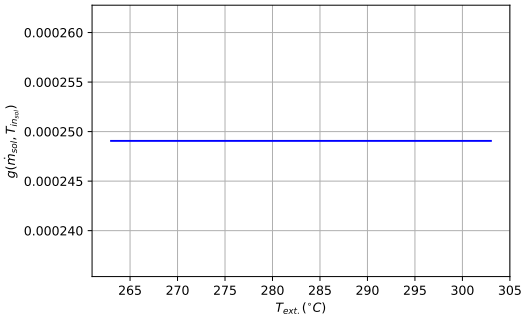

D.2. Water cooled system

Decay-heat fraction

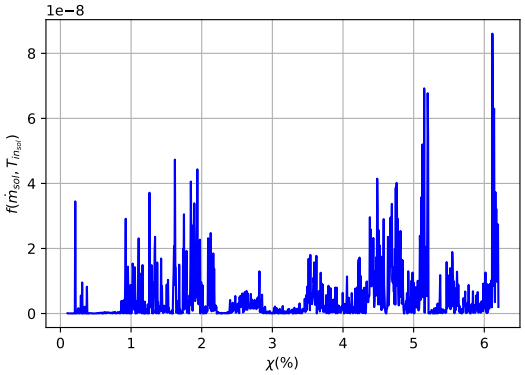

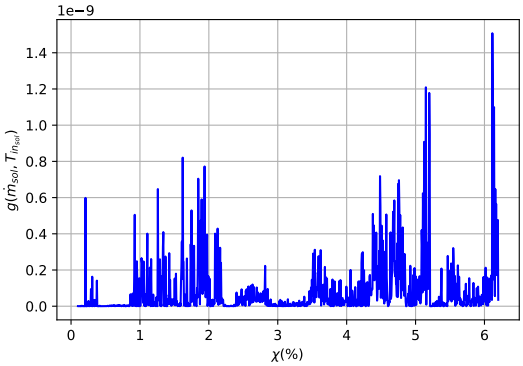

Heat transfer coefficient

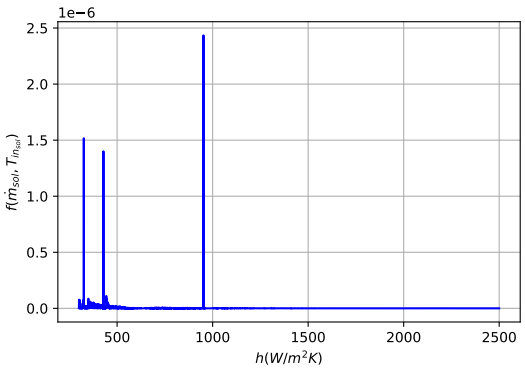

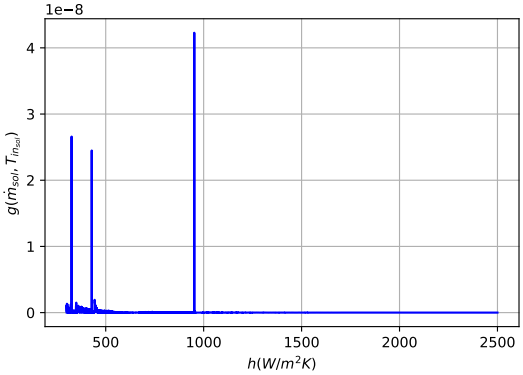

Heat exchanger length

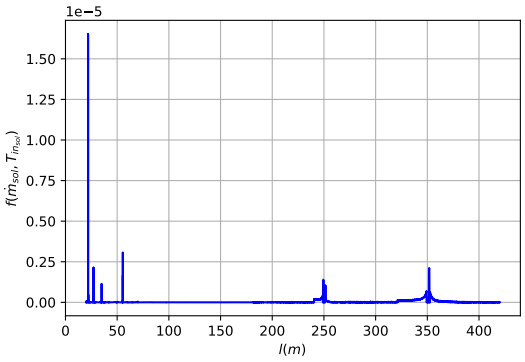

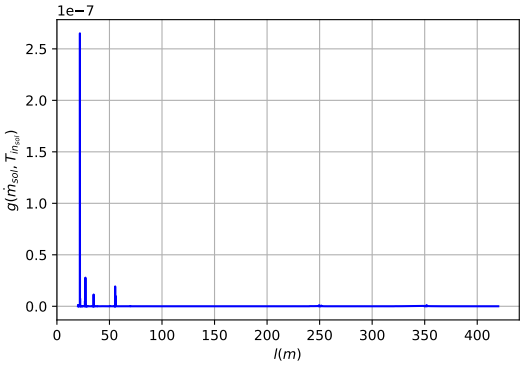

D.3. Propyleneglycol cooled system

Decay-heat fraction

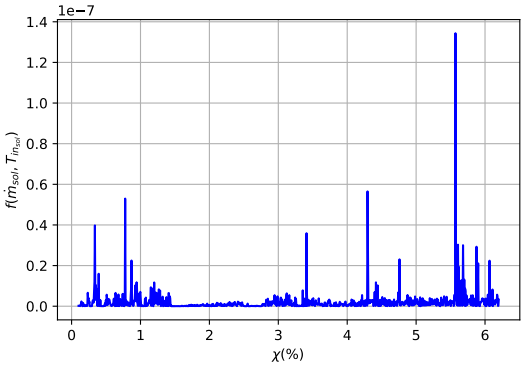

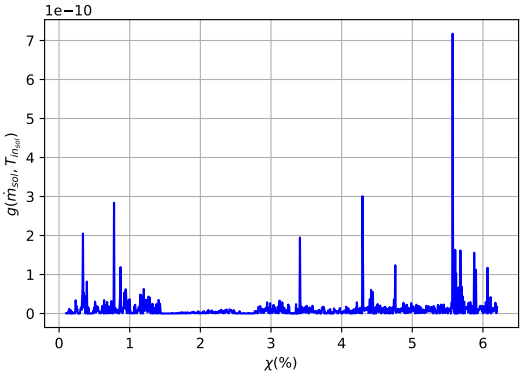

Heat transfer coefficient

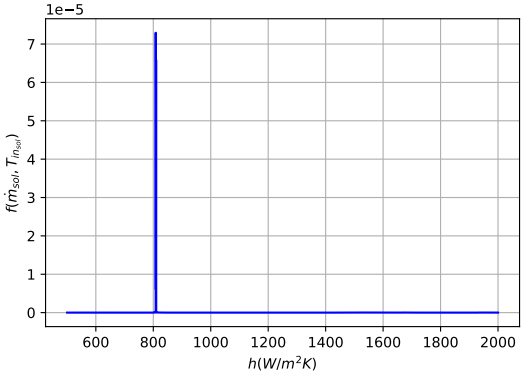

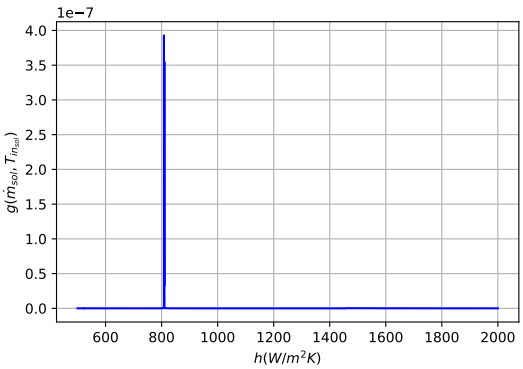

Heat exchanger length

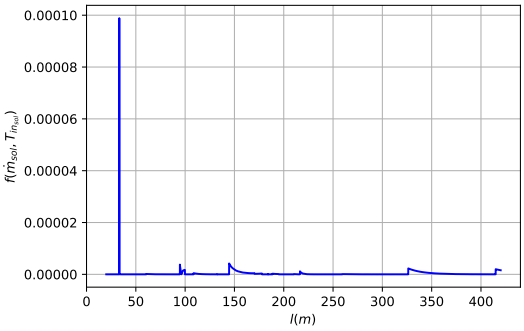

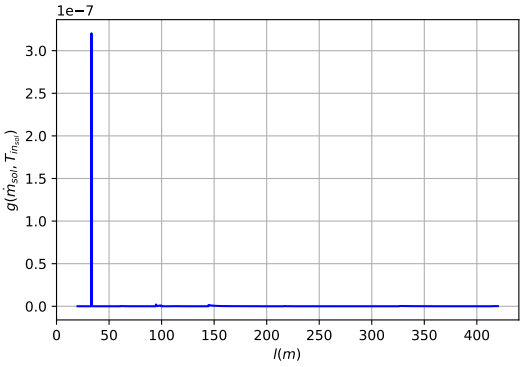

D.4. Carbon dioxide cooled system

Decay-heat fraction

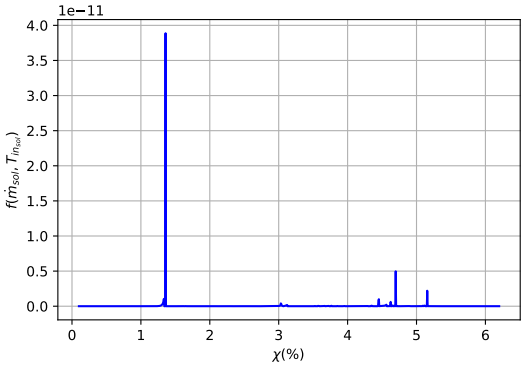

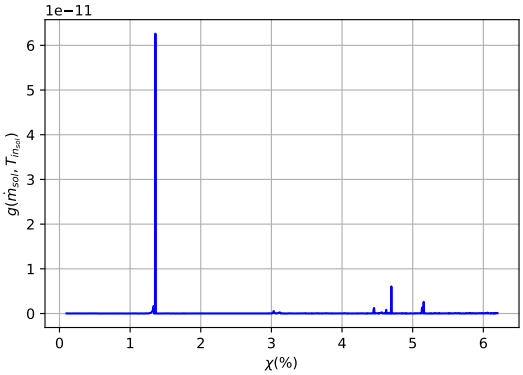

Heat transfer coefficient

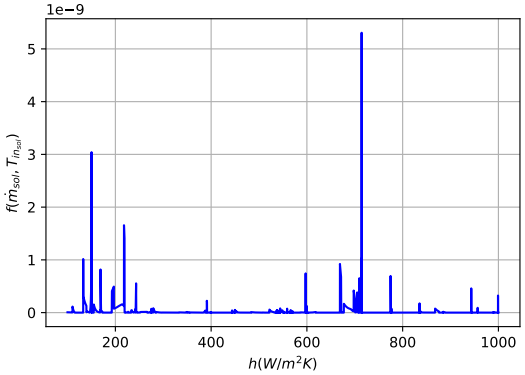

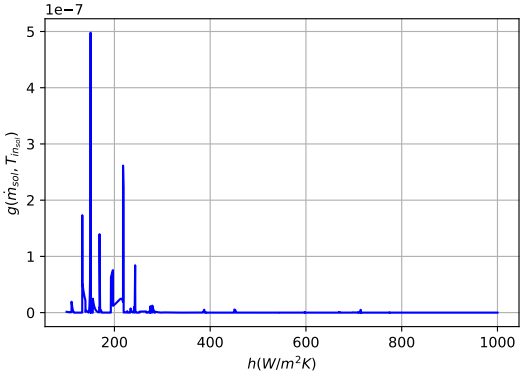

Heat exchanger length